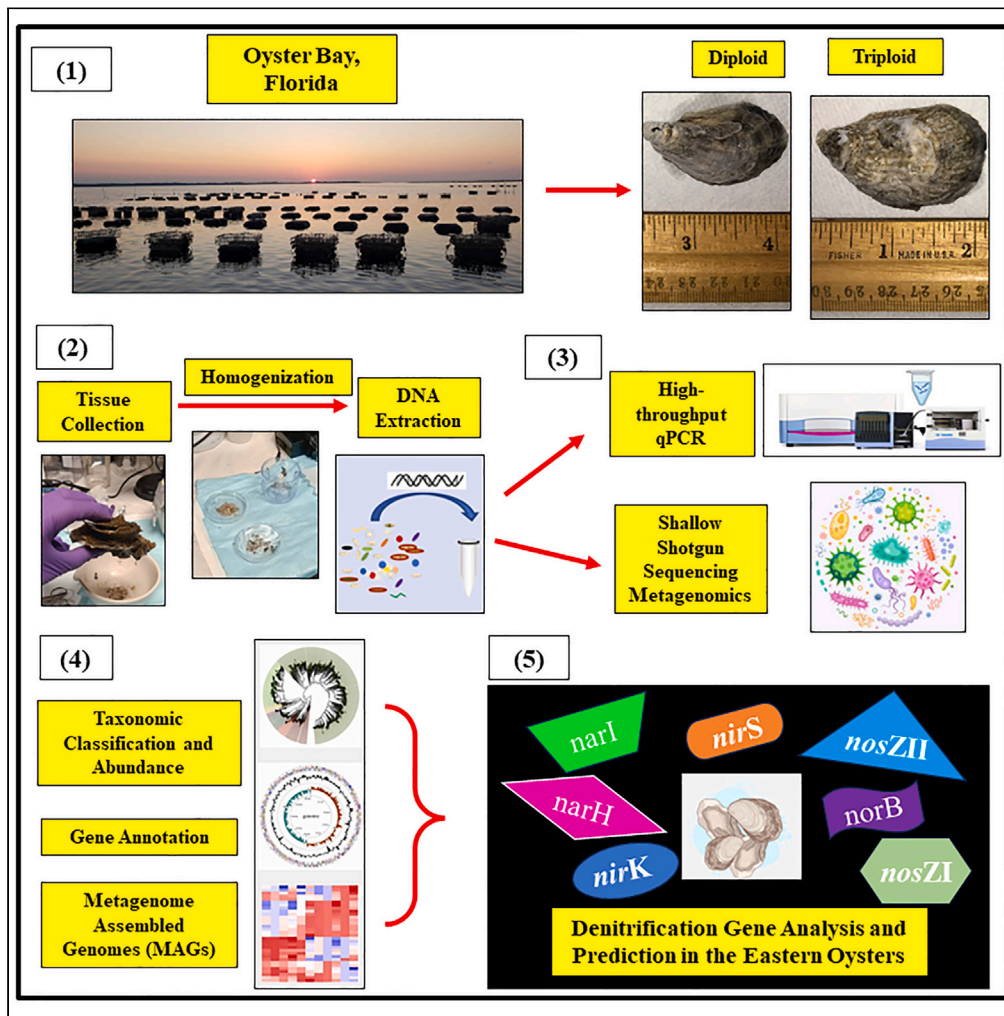


Article

# A seasonal study on the microbiomes of Diploid vs. Triploid eastern oysters and their denitrification potential



Ashish Pathak,  
Mario Marquez,  
Paul Stothard, ...,  
Xin-Yuan Zhou,  
Charles H. Jago, Jr.,  
Ashvini Chauhan

ashvini.chauhan@fam.u.edu

Highlights

*Psychrobacter* genus predominated in farmed diploid and triploid eastern oysters

Reconstructed MAGs of *Psychrobacter* spp. contained several denitrification genes

QMEC analysis indicated predominance of carbon (C) and nitrogen (N) cycling genes

The *nosZII* denitrifier clade was overrepresented regardless of ploidy and seasons



## Article

## A seasonal study on the microbiomes of Diploid vs. Triploid eastern oysters and their denitrification potential

Ashish Pathak,<sup>1</sup> Mario Marquez,<sup>2</sup> Paul Stothard,<sup>3</sup> Christian Chukwujindu,<sup>4</sup> Jian-Qiang Su,<sup>5</sup> Yanyan Zhou,<sup>5</sup> Xin-Yuan Zhou,<sup>5,6</sup> Charles H. Jagoe,<sup>1</sup> and Ashvini Chauhan<sup>1,7,\*</sup>

## SUMMARY

**Oyster reefs are hotspots of denitrification mediated removal of dissolved nitrogen (N), however, information on their denitrifier microbiota is scarce. Furthermore, in oyster aquaculture, triploids are often preferred over diploids, yet again, microbiome differences between oyster ploidies are unknown. To address these knowledge gaps, farmed diploid and triploid oysters were collected over an annual growth cycle and analyzed using shotgun metagenomics and quantitative microbial elemental cycling (QMEC) techniques. Regardless of ploidy, *Psychrobacter* genus was abundant, with positive correlations found for genes of central metabolism, DNA metabolism, and carbohydrate metabolism. MAGs (metagenome-assembled genomes) yielded multiple *Psychrobacter* genomes harboring *norB*, *narH*, *narI*, and *nirK* denitrification genes, indicating their functional relevance within the eastern oysters. QMEC analysis indicated the predominance of carbon (C) and nitrogen (N) cycling genes, with no discernable patterns between ploidies. Among the N-cycling genes, the *nosZII* clade was overrepresented, suggesting its role in the eastern oyster's N removal processes.**

## INTRODUCTION

Oysters are consumed widely on a global scale due to their unique taste as well as nutritional value, which is high in proteins, polyunsaturated fatty acids (PUFA), vitamins, and minerals.<sup>1,2</sup> According to estimates from 2020, U.S. oyster landings totaled 9 million kg,<sup>2-4</sup> with an annual value of almost \$187.2 million USD.<sup>3-5</sup> *Crassostrea virginica*, the eastern oyster or the American oyster, accounts for as much as 75% of all commercialized oysters in the United States, with the coastal regions of Florida, Texas, Louisiana, Mississippi, and Alabama, contributing to more than 60% of the total production.<sup>5</sup>

Oysters also provide ecosystem services, including maintaining water quality and sustaining estuarine habitats<sup>6</sup> and thus, are recognized as keystone species across North American coasts from Florida to Maine. In fact, a single adult oyster can filter as much as 50 gallons of estuarine water per day,<sup>7</sup> which is a significant bioextractive mechanism resulting in a net positive impact on water quality by way of removing particulate material and nutrients, especially the microbially mediated removal of nitrogen (N), thus mitigating algal blooms and fish kills. In this regard, oyster aquaculture has been recognized as a long-term tool to mitigate coastal eutrophication problems.<sup>8-10</sup>

Despite the significance of oysters as stated above, their populations continue to decline with up to 85% of oyster habitats decimated globally, as a function of overharvesting, habitat fragmentation, decreased water quality, shifts in estuarine water salinity, and diseases.<sup>11,12</sup> According to Kirby,<sup>13</sup> oyster fisheries expanded and collapsed in a linear sequence along eastern North America, western North America, and eastern Australia. To address this, oyster aquaculture is being used to meet the continued oyster demand, especially by applying newer genomics techniques, such as inducing polyploidy.<sup>14</sup> Note that triploid oysters grow faster and produce higher yields relative to diploids due to partial sterility, higher heterozygosity, and different energy allocations for growth and gametogenesis,<sup>15</sup> and can be marketable year-round.<sup>16</sup> Moreover, triploid oysters appear to be less sensitive to environmental changes and stressors. According to Qin et al. 2019, the survival rate of triploid oysters was higher than the diploid oysters in warmer months, suggesting that the triploid oysters are more stable with environmental variations. Moreover, triploid oysters have a lower mortality rate in the face of stressors leading to mortality outbreak, including physiological

<sup>1</sup>School of the Environment, Florida A&M University, 1515 S. Martin Luther King Boulevard, Tallahassee, FL 32307, USA

<sup>2</sup>Texas Sea Grant College Program, 4115 TAMU Eller O&M 306, Texas A&M University, College Station, TX 77843, USA

<sup>3</sup>Department of Agricultural, Food and Nutritional Science, University of Alberta, General Services Bldg, Edmonton, AB T6G 2H1, Canada

<sup>4</sup>Material & Energy Technology Department, Projects Development Institute, Emene Industrial Layout, Enugu-Nigeria 400104

<sup>5</sup>Fujian Key Laboratory of Watershed Ecology, Key Laboratory of Urban Environment and Health, Institute of Urban Environment, Chinese Academy of Sciences, Xiamen 361021, China

<sup>6</sup>University of Chinese Academy of Sciences, Beijing 100049, China

<sup>7</sup>Lead contact

\*Correspondence: [ashvini.chauhan@famu.edu](mailto:ashvini.chauhan@famu.edu)

<https://doi.org/10.1016/j.isci.2024.110193>



stress associated with gonadal maturation, pathogens, pollutants, aquaculture practices, and elevated temperature.<sup>17</sup> Given these advantages, triploid oysters account for most of the commercially produced oysters in the US.

Regardless of ploidy, filter feeding behavior fosters the colonization of the oyster's nutrient-rich mucosa and digestive organs with a plethora of diverse estuarine microbiota-which are either permanently associated with the bivalve oyster, referred to as the autochthonous bacterial communities,<sup>18–20</sup> or can be transient, called as the allochthonous bacteria-communities that are ingested through filter feeding and simply making their way through the bivalves gills and digestive organs. The autochthonous "core" microbiota can forge a mutually beneficial symbiotic relationship with their bivalve host organism; however, a universal "core" pertaining to host-microbe interactions remains unclear.<sup>21</sup> Furthermore, it also remains to be known whether the triploid oysters, due to their larger size, filter a higher biomass of bacteria from the water column and accumulate larger concentrations and/or diversity of beneficial or pathogenic mortality inducing bacteria, thus represented with a different "core" microbiome compared to the diploids. To this end, De Deckar et al.<sup>22</sup> reported a higher susceptibility of triploid oysters to the pathogenic *Vibrio* bacteria relative to their diploid counterparts.

It was Colwell and Liston that first suggested the existence of a defined commensal flora in oysters dating back to 1960.<sup>23</sup> Zurel et al.<sup>24</sup> have shown a conserved seasonal association between the Chama-associated oceanospirillales group (CAOG) of bacteria with oysters, likely representing a symbiotic association. Trabal et al.<sup>25</sup> reported symbiotic host-bacteria relationships during different growth phases of two oyster species- *Crassostrea gigas* and *Crassostrea corteziensis*. Such symbionts may assist in the digestion processes, as has been demonstrated in the larvae of *Crassostrea gigas*<sup>26</sup> and may also supply the bivalve host with vitamins and amino acids that serve as growth factors-as shown in the Pacific vesicomid clam- *Calyptogena magnifica*.<sup>27</sup> Moreover, certain symbiotic bacteria can even protect their host from pathogens by either producing antimicrobial agents, or by growing in high densities that prevents colonization by other strains.<sup>28</sup> More recently, Sakowski et al.<sup>29</sup> discovered that up to 33% of the microbiota from the extrapallial fluid, responsible for shell formation, were autochthonous to *C. virginica*. Interestingly, the extrapallial fluid-associated microbiota were reported to be rich in functions related to dissimilatory nitrate reduction, nitrogen fixation, nitrification, and sulfite reduction. Banker and Vermeij<sup>30</sup> reported that sulfate reduction bacteria (SRB) play significant roles in calcification, but they may not be the only bacteria involved in this process. Moreover, the sulfate and nitrate reduction were proposed to have a synergistic effect on calcium carbonate precipitation and thus likely impacting shell formation.<sup>29</sup> It was also previously shown by Braissant et al.<sup>31</sup> that SRBs can produce exopolymeric substances (EPS) which can serve as a site for CaCO<sub>3</sub> precipitation, and that the calcifying ability can be enhanced by an increase in alkalinity due to the reduction in sulfate ions. Furthermore, most calcifying bacteria are also actively involved in nitrate reduction.<sup>32</sup> In this regard, beneficial oyster microbiota likely enhances their host health, thus promoting growth and longevity. To further tease out the transient (allochthonous) oyster microbiota from the resident ones, a flexibility score (FS) was recently developed, which showed that the gill tissues harbor a diverse range of resident bacteria.<sup>18</sup>

The major bacterial phyla of the eastern oysters are as follows: Proteobacteria, Cyanobacteria, Bacteroidia, Mollicutes, Bacteroidetes, Tenerecutes and Firmicutes.<sup>29,33–41</sup> A consensus on the genus level "core" and possibly the resident or autochthonous microbiome of eastern oysters is lacking, but the following bacteria, in addition to *Vibrio* species, have been identified to be dominant groups: *Mycoplasma*, *Pseudomonas*, *Burkholderia*, *Bacteroides*, *Lactobacillus*, *Acetobacter*, *Allobaculum*, *Ruminococcus*, *Nocardia*, and *Oceanospirillales*.<sup>18,42</sup> It is noteworthy that the bacterial communities within the eastern oyster and its specific niches, such as the mantle fluid, gills, digestive system, gut, extrapallial fluid, and hemolymph have been found to be distinctly different than the surrounding water or sediment communities.<sup>18,20,29,34,37</sup> In one previous study conducted on the wild type and farmed eastern oysters, we found Cyanobacteria accounting for 50–75% of the total microbial communities, based on 16S rRNA amplicon metagenomics.<sup>43</sup> In another microcosm-based study related to the Deepwater Horizon oil spill, *Pseudomonas* spp. were found to be the dominant oyster-associated bacteria.<sup>43–46</sup> More recently, our metagenomics survey of the eastern oysters indicated the dominance of *Lactobacillus*, *Burkholderia*, *Bradyrhizobium*, *Afiopia*, and *Delftia* bacterial groups with lower representations of *Psychrobacter* spp. Additionally, *Mycoplasma*, which has been previously suggested as one of the autochthonous bacteria in eastern oysters, was also identified (unpublished data).

One major ecosystem service associated with the oysters relates to enhancing water quality by the utilization of the dissolved nitrogen by both oysters and their microbial communities. Specifically, N assimilated into oyster shells and tissues is removed from the estuarine systems via harvesting or burial.<sup>47</sup> Oyster feces and pseudofeces contribute organic material to sediments, potentially enhancing denitrification processes. Denitrification is a four-step reduction of nitrate (NO<sup>3-</sup>) to N<sub>2</sub> via nitrite (NO<sub>2</sub>), NO and N<sub>2</sub>O and eventually to nitrogen gas.<sup>29,48</sup> At the genetic level, denitrifying bacteria harbor genes in operonic clusters that encode functions for the reduction of nitrate (*narG/napA*), nitrite (*nirS/nirK*), nitric oxide (*norB/norC*), and nitrous oxide (*nosZ*).<sup>49</sup>

The above stated background led us to the following overarching question - what are those suits of environmentally relevant biogeochemical functions, such as nitrogen cycling, that are performed by the eastern-oyster associated microbiome communities? To address this, we applied shallow shotgun sequencing (SSS) based metagenomics, which is a reliable method to understand both taxonomic and functional gene shifts in complex environmental samples.<sup>50</sup> To augment findings obtained from metagenomics, we applied the recently developed method of "Quantitative Microbial Elemental Cycling (QMEC)", a high-throughput quantitative PCR (HT-qPCR) technique for estimating microbial gene copy numbers engaged in the critical steps of carbon (C), nitrogen (N), phosphorus (P), and sulfur (S) cycling as well as methane metabolism.<sup>51</sup> Given that the commercially grown eastern oysters are triploid variants that originated from the wild-type diploids, and that their microbially mediated functions likely shift with time, both diploid and triploid eastern oysters were collected monthly over an annual growth period to: 1) conduct shotgun metagenomics and identify native autochthonous microbial groups; 2) evaluate the microbial gene functional shifts occurring within the microbiome; and 3) evaluate microbially mediated CNPS biogeochemical cycling by applying the QMEC method.

## RESULTS AND DISCUSSION

### Characterization of sampled oysters and quality control on shotgun metagenome sequences

At the start of the growing period, diploid oysters ranged from 21 to 35 mm in height and 1–3 g in weight; triploid oyster heights were 12–27 mm and weights were 0.5–1 g. After one year of growth, diploids were 85–95 mm in height and 54–91 g in weight, and triploids were 71–105 mm in height and 75–110 g in weight (cultured oysters are considered harvestable when height >76 mm).

For the metagenomic analysis, 10 diploid and 10 triploid oysters were collected at each time point and pooled separately to generate duplicates A and B. Shallow shotgun sequences (SSS) obtained from  $n = 6$  each of diploid and triploid oysters, collected in duplicates (labeled as A or B), yielded over 113.2 million raw reads and 98.3 quality-filtered reads (Figure SI-1). Around 34.3 (34.8%) and 0.5 million (0.51%) of the quality-filtered reads were assigned to the oyster host (*Crassostrea virginica* genome v3.0 (Accession number GCF\_002022765.2) and the human genome (Genome Reference Consortium Human ref. 37), which were removed prior to further processing.

One goal of this study was to examine the eastern oyster microbiome over an annual growth cycle with oysters collected every month, rather than using random grab samples, which are appropriate only to provide a quick snapshot of bacterial communities but are not sensitive in the assessment of the eastern oyster's autochthonous microbiome communities. Once the "core" microbiome of the eastern oyster is better understood, specific studies can be conducted to identify those microbial groups that are specific to beneficial functions such as maintenance of oyster growth, overall health, and productivity. To this end, regardless of seasons or ploidy, the eastern oysters were found to be predominantly colonized by bacteria, as shown by 93.4% of sequences that were annotated to the bacterial domain, followed by eukaryotes (5.64%), archaea (0.76%) and viruses (0.25%), respectively. Among bacteria, a total of 36 phyla were identified across all the samples with the top 5 phyla represented by *Pseudomonadota* (58%; former *Proteobacteria*); *Bacillota* (11%; former *Firmicutes*); *Bacteroidota* (7%; former *Bacteroidetes*); *Cyanobacteria* (6%) and *Actinomycetota* (3%; former *Actinobacteria*), respectively. *Pseudomonadota* are metabolically and ecologically diverse and are commonly found in many environments, including animal hosts; some proteobacterial groups are also pathogenic. These findings are in line with other previous studies, which show the dominance of proteobacterial lineages in oysters.<sup>29,36,40,43,52–54</sup> *Pseudomonadota* also likely play important functional roles in the eastern oysters, such as nitrogen cycling.<sup>9,38,48</sup> Furthermore, proteobacterial members can also metabolize cellulose and agar-major components of the oyster's phytoplanktonic diet, and hence colonize bivalve gastrointestinal tracts,<sup>25</sup> providing nutrients and bioactive growth factors to their oyster hosts.<sup>19,24,39,55–57</sup>

Among proteobacterial members, the gamma-proteobacterial class was the most abundant, as also shown by,<sup>36</sup> followed by alpha- and delta proteobacteria. These proteobacterial groups are typically found in high numbers in marine environments, and are likely concentrated within the oysters due to their filter-feeding activity.<sup>25,36,58,59</sup> Also, gamma-proteobacteria have been frequently detected in both healthy or diseased shellfish including oysters<sup>28</sup> and as endosymbionts from the gills or gonads of different bivalve species.<sup>60,61</sup> Therefore, gamma-proteobacteria are likely to be autochthonous to oysters,<sup>62</sup> given their ubiquity with oysters and their surrounding environment.<sup>29,62</sup>

As shown in Figure 1A, the top 3 gamma-proteobacterial genera included *Psychrobacter* (34%); *Pseudomonas* (3.2%); and *Pseudoalteromonas* (2.7%). Besides these gamma-proteobacteria, cyanobacterial *Synechococcus* spp., from class Cyanophyceae was the second most abundant bacteria (3.6%). These bacterial genera likely constitute the "core" microbiomes in the eastern oysters analyzed in this study, using the MicrobiomeAnalyst pipeline, at a threshold of 10% sample prevalence and 0.01% relative abundance (Figure 1B). The top 10 bacterial "core" genera were *Psychrobacter*, *Synechococcus*, *Pseudomonas*, *Clostridium*, *Pseudoalteromonas*, *Mycoplasma*, *Bacillus*, *Staphylococcus*, *Vibrio* and *Cyanobium*, (Figure 1B). *Psychrobacter* represented 6 out of the dominant 10 species found in these eastern oysters, including *P. sp.* P11F6; *P. sp.* 28M-43; *P. sp.* P11G3 (data not shown).

*Psychrobacter* are known to typically thrive in colder marine ecosystems (Bowman, 2006), such as glacial ice,<sup>63</sup> sea ice,<sup>64</sup> permafrost,<sup>65</sup> as well as found associated with deep sea animal host species e.g., sponge, porpoise, crab, krill, seal, and cyanobacterial mats.<sup>66–69</sup> However, warmer niches have also been found to be colonized by *Psychrobacter* spp. including humans, lambs, and fecal materials from pigeons.<sup>66,68</sup> In a recent genomic and phenotypic comparison of an extensive cohort of *Psychrobacter* spp. Welter et al.<sup>66</sup> showed that the *Psychrobacter* can be delineated into two growth profiles: the "flexible ecotype" (FE) group that could grow in temperatures between 4°C and 37°C, and the "restricted ecotype" (RE) group that grew between 4°C and 25°C temperature. The dominant *Psychrobacter* spp. in this study are closely related to those isolated from marine Arctic environments, indicating that the eastern oyster surveyed in this study likely harbor the RE *Psychrobacter* ecotypes. Proliferation of psychrotrophic bacteria that create conditions for seafood spoilage by hydrolysis of proteins and lipids in oyster tissues, producing malodorous compounds and toxic byproducts,<sup>70</sup> can be a cause for concern. Beneficial probiotic properties of *Psychrobacter* have also been reported in some studies, such as enhancing growth and survival of shrimp larvae,<sup>71</sup> and by enhancing autochthonous microbiomes and protection from bacterial pathogens (e.g., *Vibrio* sp.) in Atlantic cod.<sup>72–74</sup> Therefore, it may be possible that *Psychrobacter* spp. are beneficial to eastern oysters in a similar manner. Interestingly, it has been reported that oyster processing, including refrigeration, storage, and depuration at 10°C, caused a shift in the predominant *Vibrio* species that are characteristic of freshly harvested oysters, toward psychrotrophic bacteria consisting of *Pseudomonas* spp., *Aeromonas* spp., *Shewanella* spp., and *Psychrobacter* spp..<sup>75</sup> Therefore, further research on the dominance of *Psychrobacter* species in eastern oysters should be conducted to evaluate whether these species provide benefit(s) to their oyster host or represent an underexplored agent of oyster spoilage processes.

In this regard, some species of *Psychrobacter*, mainly *P. sanguinis*, *P. phenylpyruvicus*, *P. faecalis*, and *P. pulmonis* are known to cause opportunistic infections in mammals,<sup>76,77</sup> which needs to be further investigated. Human infections from consuming raw or undercooked shellfish containing a higher abundance of *Psychrobacter* species has not been demonstrated, nor has the predominance of *Psychrobacter* been shown for eastern oysters prior to this work. Given that the *Psychrobacter* identified in the eastern oysters in this study appear mainly to be the RE ecotypes, it is likely that they can mount mammalian infections that require warmer temperatures, however, this aspect remains

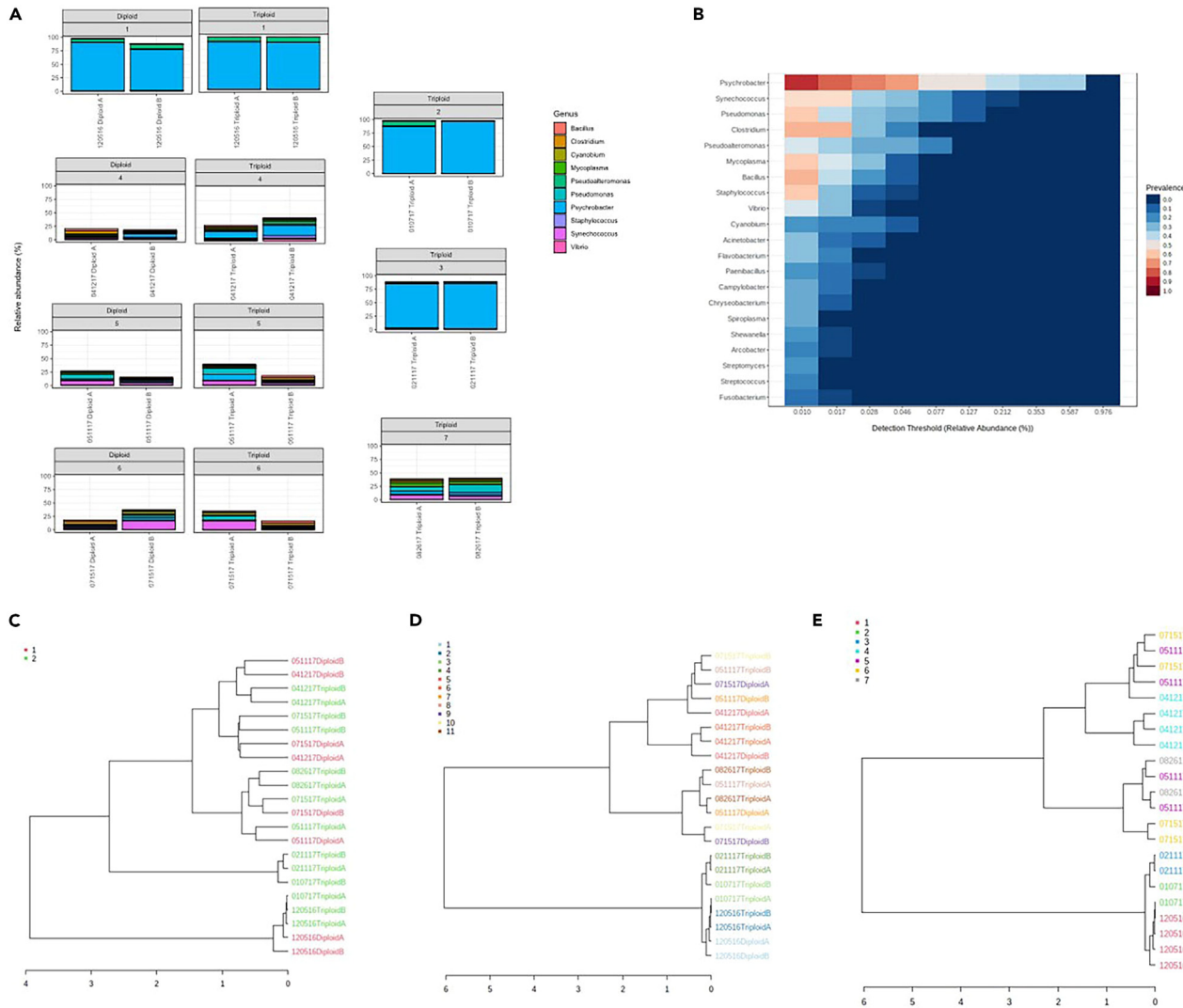


**Figure 1. Taxonomy and dendrogram analysis of the eastern oyster's microbiome using shallow shotgun metagenomics analysis**

Shown are the bacterial genera-level taxonomic groups identified in diploid eastern oyster vs. triploids, sampled in duplicates (each time point is labeled as A or B), over an annual cycle. Specifically, shown are (A), metagenome sequences grouped as originating from either diploid or triploid oysters, regardless of sampled time; (B) core microbiomes identified in the eastern oyster, regardless of ploidy or sampled seasons; (C) dendrogram analysis conducted on bacterial genus-level data obtained from diploid vs. triploid populations with group 1 containing diploids and group 2 containing triploids; (D) dendrogram analysis conducted on samples binned as a function of sampled time period and ploidy was ignored; (E) dendrogram analysis conducted on samples grouped as a function of collection time period: group 1 (December 2016); group 2 (January, 2017); group 3 (February, 2017); group 4 (April, 2017); group 5 (May, 2017); group 6 (July, 2017); group 7 (August, 2017), respectively.

unclear. As stated before, genomic analysis has recently suggested that *Psychrobacter* ecotypes likely evolved from a mesophilic common ancestor, which presents a unique opportunity to delineate the evolutionary mechanisms of the eastern oyster associated *Psychrobacter* species as a function of their estuarine habitats.

When oysters were compared over different time points, a decline in bacterial abundances was observed from April to August, representing the warmer season. For example, proteobacterial abundances were predominant at an average of 97% between December 2016 to February 2017 but declined to 36% from April to August 2017. Along these lines, it was recently shown for the Australian Pacific oysters (*Crassostrea gigas*) that temperature strongly correlated to their microbiomes and that microbial diversity increased in winter relative to summer timepoint.<sup>43</sup> Besides, temperature is one of the factors that influences the survival rate of oysters with high temperature leading to decrease thermal tolerance, reduced growth, survival, and filtration rates.<sup>78</sup> Moreover, elevated temperature leads to oyster spawning and spawned oysters are highly vulnerable to temperature stress.<sup>79</sup> Other stressors such as increased ocean acidification and salinity equally impact the strength, reproduction, growth, and oysters' mortality<sup>78</sup>. However, it is highly likely that low temperature favored the observed increase

of the psychrotrophic *Psychrobacter* species in this study (Figure 1B). Interestingly, dendrogram analysis conducted on bacterial metagenomes revealed less affiliation with regards to ploidy; conversely, seasonal changes appeared to have a stronger influence in structuring the oyster microbiome (Figures 1C–1E). Specifically, when metagenomes were grouped as originating from either diploid or triploid oysters (Figure 1C), a total of 6 clusters representing different time periods were observed. The general trend was that the metagenomes from the colder months—December, January, and February, clustered together, as did those from the warmer months of April, May, July and August. When sequences were grouped as a function of sampled time and ploidy was ignored, 5 clusters emerged, and again, the season exerted a stronger influence in driving the bacterial communities, relative to ploidy (Figure 1D). As a third option, when samples were grouped as a function of the sampled time, 6 clusters were observed which clearly shows seasonal impacts to be in the major factor structuring the oyster-associated microbiomes, when compared with ploidy (Figure 1E). This finding is noteworthy because most studies on the eastern oysters have been conducted using samples collected at random times during the year,<sup>35,37–40</sup> and even those that were samples on a spatiotemporal basis focused on pathogen dynamics such as *Vibrio* and their occurrence in the eastern oysters.

The other two main bacterial genera identified were *Synechococcus* and *Pseudomonas* spp. (Figure 1A and 1B). *Synechococcus* spp. are commonly found in estuarine waters and have also been reported from the digestive gland *C. gigas*, as well as connective tissue, mantle, and gonad of oysters.<sup>80</sup> Our previous studies along with several others have demonstrated pseudomonads to be a major bacterial group in the oysters.<sup>44–46</sup> Notably, some pseudomonads can be opportunistic pathogens and have been found in spoiled oysters.<sup>1,53,81</sup> To provide further insights into the metabolic traits of *Pseudomonas* species from the eastern oysters, we conducted whole genome sequencing (WGS), comparative genomic analysis and BIOLOG-based physiological assessments on isolates obtained from the eastern oysters.<sup>82</sup> Interestingly, strains that were isolated from the mantle fluid [(*P. stutzeri* (MF28))] and tissues [(*P. alcaligenes* (OT69)), were metabolically versatile relative to those isolates obtained from the overlaying oyster bed water column [(*P. aeruginosa* (WC55)). Specifically, *P. aeruginosa* (WC55) preferred polymers over other carbon sources, while *P. stutzeri* (MF28) responded better to carbohydrates, while *P. alcaligenes* (OT69) showed similar metabolic responses to both polymers and carbohydrates, respectively. Additional studies are required to ascertain whether the eastern oyster associated *Pseudomonas* spp. provide a beneficial service to the host, such as the bioremediation of marine pollutants and providing growth promoting vitamins or mediate spoilage via their pathogenic functions.

Though not the main purpose of this study, we also analyzed the archaeal members in the eastern oyster shotgun metagenomes. Archaea are a small fraction of the microbial communities in oysters,<sup>18</sup> if not present at all.<sup>36</sup> Similarly in our study, archaea were represented at only 0.76% in the taxonomic annotation; with dominance of Euryarchaeota (41%) and Thaumarchaeota (24%), respectively (data not shown). The oyster-associated archaeal genera mainly belong to *Methanosarcina* (12%) and *Nitrosopumilus* (10%). Based on the underrepresentation of archaeal communities, it is likely that conditions for the proliferation of this group, such as anaerobiosis, were likely not present in the oysters analyzed in this study.

### Alpha and beta-diversity analysis

The bacterial genus level data were statistically evaluated using Shannon's index for differences potentially driven by seasons and ploidy using alpha and beta diversity analysis. Samples were assigned to 7 different groups based on the collection dates as stated earlier, and some low sequence samples were removed from the analysis. Regardless, this represents a good snapshot of the oyster-associated microbiomes over an annual cycle. Shannon's diversity, shown in Figure 2A, was significantly higher at later sampling timepoints but bacterial diversity in diploids and triploids was not different, possibly due to low replication (although *p*-value for genotypes was 0.056). Alpha diversity analysis revealed that warmer months had increased diversity relative to colder months (Figure 2B). It is widely accepted that warmer temperatures increase marine bacterial abundances,<sup>83</sup> which goes well with our observation of enhanced bacterial biomass in the oyster samples collected in the warmer season.

Beta diversity, which is the diversity between different samples and significance testing was also conducted as shown in Figure 3. Similar to the alpha diversity analysis, beta diversity also revealed that the microbiomes were more similar in oysters sampled in the colder months of December–February than those sampled in warmer months (Figure 3A and 3B), as has also been recently shown for Australian oysters and mussels.<sup>34</sup> Microbiomes did not differ between diploid and triploid oysters despite the relatively larger size of the triploid oysters, as stated earlier. Note that only few studies are available to compare how ploidy impacts oysters, mostly on mortality, yields, growth rates, and susceptibility to diseases.<sup>22,84</sup> Studies on other organisms, especially fish,<sup>85</sup> found that triploids contained significantly higher cultivable gut microbiota levels, especially *Pseudomonas* spp., *Pectobacterium carotovorum*, *Psychrobacter* spp., *Bacillus* spp., and *Vibrio* spp.

### Gene functional analysis of the eastern-oyster microbiomes over an annual cycle

Functional genes annotated from the oyster shotgun metagenome sequences were organized into the SEED hierarchy (Figure 4). At broad levels (levels 1 and 2), functional profiles were very similar; smaller differences were found at lower levels (data not shown). Some differences were apparent at subsystems related to bacterial respiration and they tended to increase in later timepoints; a trend similar to the taxonomic assessment, where the latter warmer timepoints revealed a higher abundance and diversity of oyster associated microbiota. The major metabolic functions identified across oyster samples belonged to respiration and metabolism of carbohydrates, RNA, and protein.

We also conducted a permutational multivariate analysis to test for differences in taxonomic composition and gene function over an annual cycle in diploid and triploid oysters (Table SI-1). This showed that taxonomic profiles changed significantly over time, with little or no significant differences observed between genotypes (ploidy). However, post-hoc tests did not find significant differences between timepoints, which can however be due to the low number of replicates. Because we did not find differences between genotypes, we pooled

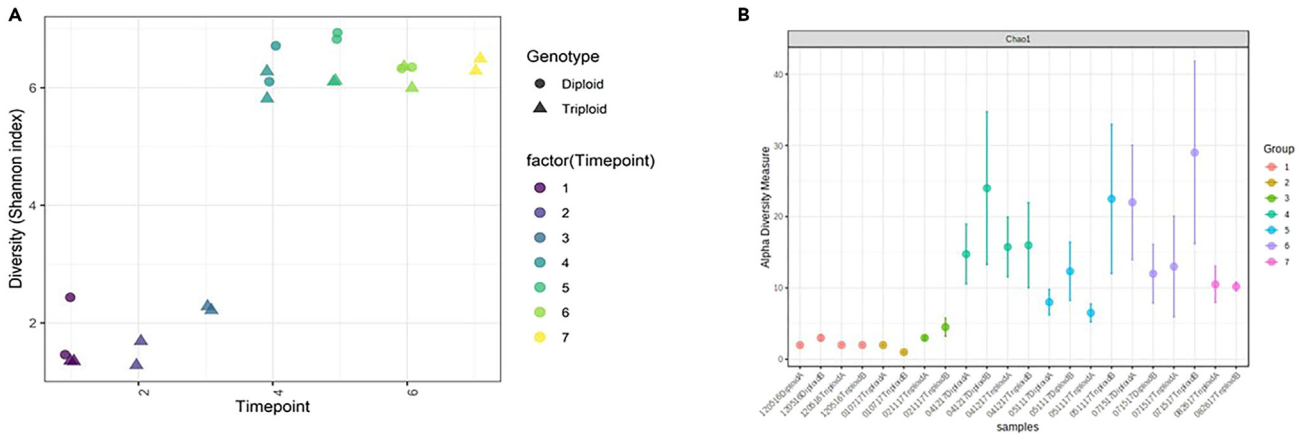


**Figure 2. Microbiome diversity analysis of the eastern oyster, across ploidy and growth time points**

Diversity analysis for each month is represented by a unique color identified in diploid eastern oyster vs. triploid populations, sampled in duplicates (each time point is labeled as A or B), over an annual cycle. Shown are (A), Shannon's diversity analysis, which was significantly higher at later sampling timepoints. No differences between genotypes (diploids and triploids) were found, probably due to low replication, though  $p$ -value for genotypes was 0.056; (B) alpha diversity calculated from taxonomic data; warmer months were higher in diversity relative to the colder months.

diploids and triploids for the general model; differences among sampling dates explained around 56% of the variation of taxonomic profiles; thus, ploidy was an insignificant factor relative to time-points. Similar to the taxonomic data, no significant differences were found for the gene functional data over the annual time-period in the sampled oysters. Perhaps if a sampling design is followed to tease out the oyster-associated autochthonous "core" microbiomes relative to the allochthonous microbiota, we would have observed a similar finding to Sakowski et al.<sup>29</sup> which showed significant enrichment ( $p < 0.05$ ) in KEGG based gene functions within the autochthonous microbiomes of the eastern oysters. It was interesting to note that Sakowski et al.<sup>29</sup> found genes associated with N-cycling, such as dissimilatory nitrate reduction, nitrogen fixation, and nitrification pathways in the autochthonous relative to the allochthonous bacterial community.

### Differential abundance of taxa and gene functions

Differential abundance testing of the bacterial taxa (top 20) and genes functions identified at the subsystem level 3 were investigated as a function of two factors-sampling timepoint and genotype (ploidy). As shown in Figures 5A and 5B, A general linear model showed several bacterial groups were significantly different when sampling began during the colder months, compared to the latter warmer months, including *Psychrobacter* and *Synechococcus* species-the two most abundant genera identified in this study (Figure 1A and 1B). Such seasonal trends in the Pacific oysters and mussels gut microbiomes have recently been published by Akter et al.<sup>29</sup> Interestingly, *Psychrobacter* species were differentially abundant in both diploids as well as triploid oysters, when analyzed separately (Figure 5B and 5C). Differential analysis of gene function data revealed several metabolic functions declining at latter timepoints (Figure 5D), which is counterintuitive because the

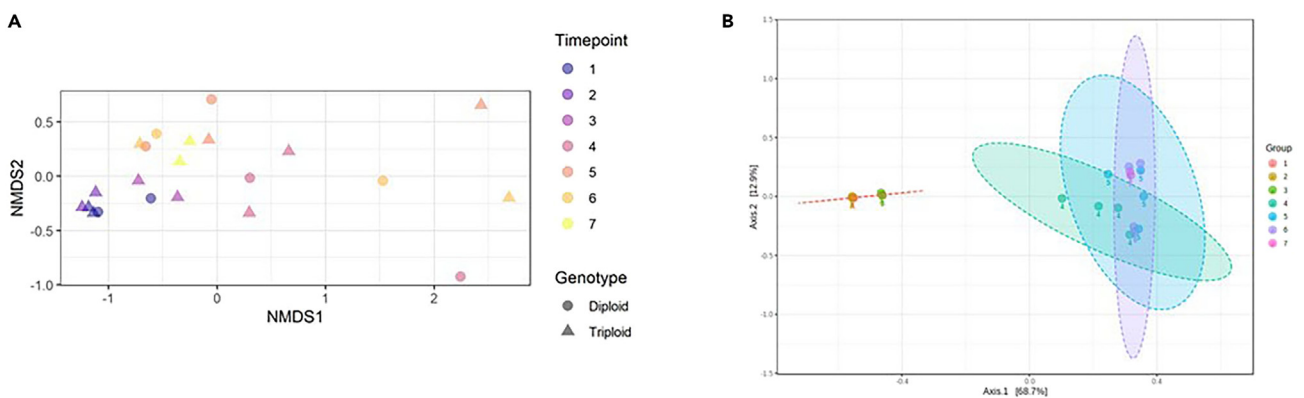


**Figure 3. Ordination of bacterial diversity at the genus level, across ploidy and growth time points**

Shown are (A), non-metric multidimensional scaling (NMDS) plot of the beta diversity using Bray-Curtis dissimilarities; (B) PCoA PERMANOVA plot of the beta diversity using Bray-Curtis dissimilarities.

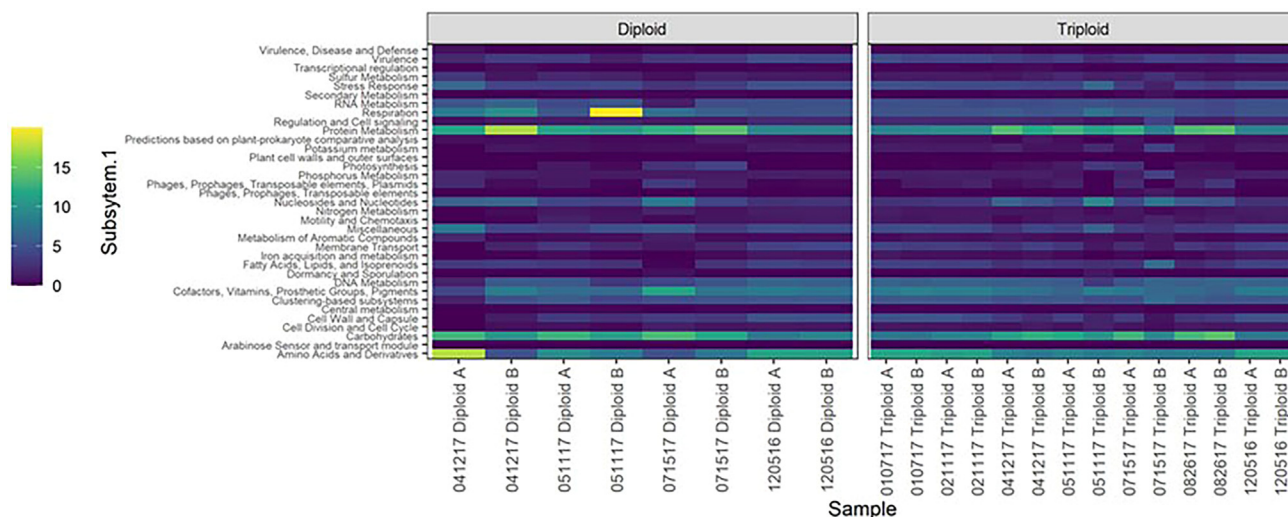


**Figure 4. Bacterial functional genes annotated from the eastern oyster metagenome sequences**

Shown are functional gene annotations at SEED functional hierarchy levels (levels 1 and 2), which were very similar. Smaller differences were found at lower levels. Some differences were apparent at subsystems related to bacterial respiration, they tended to increase in later timepoints.

bacterial taxonomic abundances increased in the mid and latter timepoints, as suggested by diversity analysis (Figure 2B). Only four gene functions were differentially abundant in diploid oysters (Figure 5E); conversely, this was not the case in triploids, where several gene abundances were differentially abundant (Figure 5F). It is unclear as to why more taxa and gene functions were differentially abundant in the triploids relative to the diploid oysters.

### Statistical correlations between bacterial taxa and gene functions

The top 10 bacterial taxa at the genus level and gene functions from SEED subsystem level 1 were analyzed statistically (Figure 6). Dendrogram analysis confirmed that eastern oyster microbiomes clustered more tightly as a function of sampling date and not from differences in ploidy (Figure 6A). Seven clusters were observed in the dendrogram plot with one outlier (sample from Dec 05, 2016, diploids) and ploidy seems insignificant relative to the sampling date for bacterial community structure in this study. The Non-metric Multi-Dimensional Scaling plots (NMDS) (Figure 6B) at a similarity at 75% and 95% revealed interesting correlations between bacterial top 10 genera and SEED subsystem level 1 features. Specifically, at the 95% similarity threshold, *Psychrobacter*, a likely member of the “core” microbiome regardless of date or ploidy status, correlated strongly to gene functions of central metabolism, DNA metabolism, and carbohydrates (Figure 6B). Other taxa that were within the 95% similarity index threshold were *Moraxella*, *Pseudoalteromonas*, *Brochothrix*, and *Halomonas*, and these correlated to gene functions of cofactors, vitamins, prosthetic groups, pigments; cell division and cell cycle; cell wall and capsule; amino acids and derivatives; dormancy and sporulation, and clustering-based subsystems. The other taxa that correlated at the 95% threshold were *Vibrio* and *Acinetobacter* with no affiliation to any of the top 10 gene functions. *Pseudomonas*, *Shewanella*, and *Flavobacterium* were not significantly correlated to other taxa or gene functions (Figure 6B). At a threshold of 75% similarity, all the above stated top 10 bacterial genera and gene functions were correlated. Based on this, it is likely that *Psychrobacter* species perform significant functional roles in the eastern oyster and thus, further studies to assess the role of this genus within the broader context of the oyster microbiome and how it intersects with oyster health and productivity are thus suggested from this study.

### Metagenome assembly, phylogenetic, and average nucleotide identity analysis

To better characterize the dominant species, metagenome assembly was performed, followed by phylogenetic analysis of select MAGs (metagenome-assembled genomes). Eleven MAGs were obtained, six of which remained after filtering based on completeness as measured using BUSCO (Table 1). Four of the six were classified as *Psychrobacter* (Figure 7), one as *Pseudoalteromonas* and one as belonging to the same family as COTS27, a bacterial symbiont of the crown-of-thorns starfish.<sup>86</sup> The MAGs consist of many contigs ( $M = 591.5$ ,  $SD = 213.4$ ) and exhibit a modest level of completeness ( $M = 51.6\%$ ,  $SD = 22.2\%$ ). The MAG SPAdes-group-0.1.fa displays a higher level of duplicated genes (8.1%), which could reflect the presence of genes from more than one species or issues with the assembly. Phylogenetic analysis of inferred protein sequences was performed to compare the *Psychrobacter* MAGs to each other and to *Psychrobacter* RefSeq assemblies available in the NCBI Assembly database. The resulting maximum likelihood tree supports that the four *Psychrobacter* MAGs are each most closely related to separate *Psychrobacter* RefSeq assemblies, and not part of a single lineage.

To complement the phylogenetic analysis, whole-genome average nucleotide identity (ANI) was calculated between each *Psychrobacter* MAGs and all *Psychrobacter* RefSeq genomes (Table 2). MAGs SPAdes-group-0.4.fa and SPAdes-group-0.5.fa exhibit high ANI (98%) with



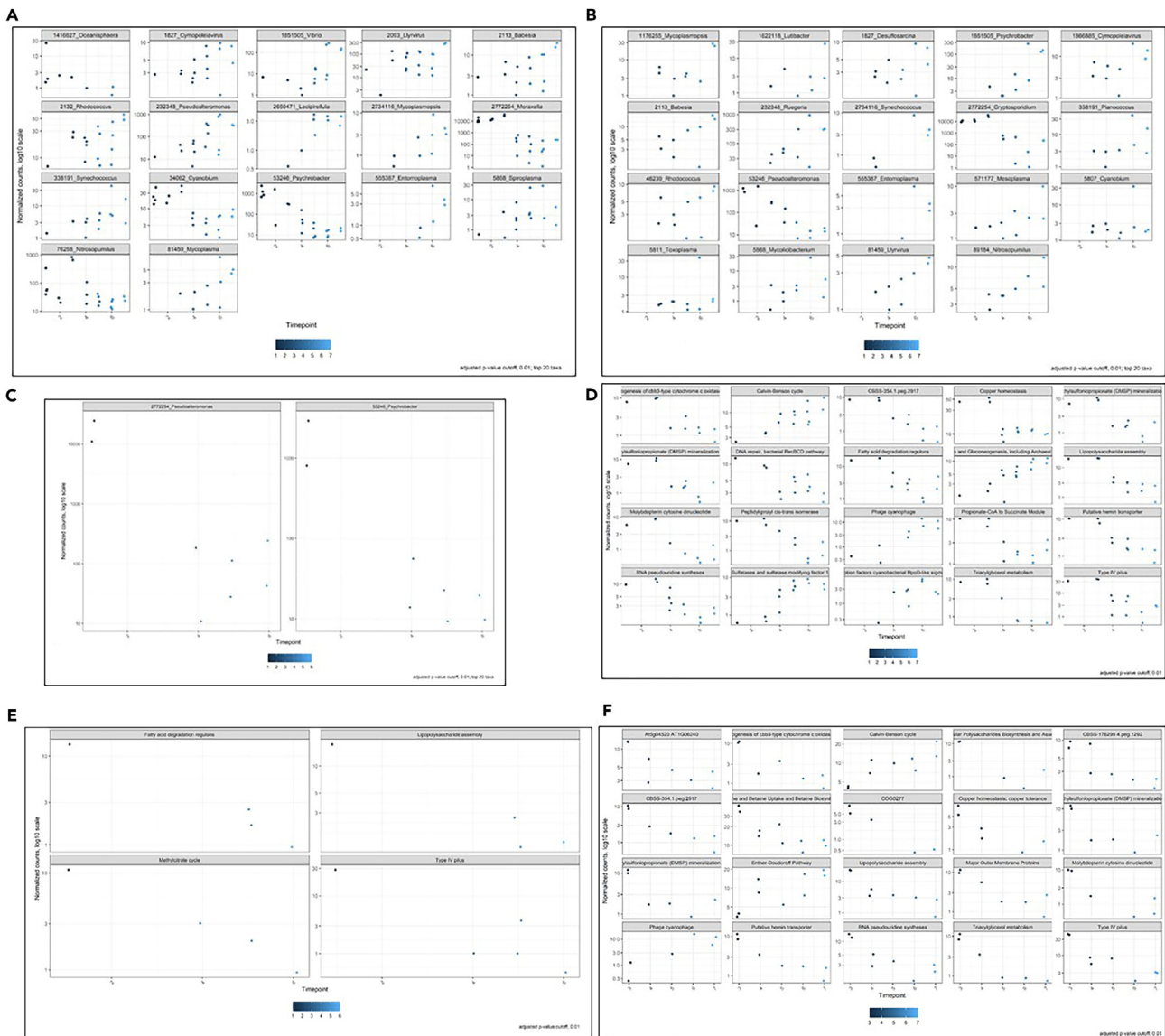


**Figure 5. Differentially abundant taxa (genus level) and gene functions (subsystem level 3) identified from the eastern oyster metagenomes across ploidy and growth time points**

Shown are (A) differentially abundant taxa using a general linear model; (B) differentially abundant taxa in diploid oysters; (C) differentially abundant taxa in triploid oysters; (D) differentially abundant gene functions using a general linear model; (E) differentially abundant gene functions in diploid oysters; (F) differentially abundant gene functions in triploid oysters, respectively.

their respective matches, and the similarity involves most of the MAG sequence (97%). These ANI values are characteristic of intra-species relationships.<sup>87</sup> SPAdes-group-0.8.fa also showed high ANI with its top match (97%) but the similarity involved just 71% of the MAG. SPAdes-group-0.1.fa exhibited a lower ANI (88%) with its top match, which is lower than the intra-species level (>95%),<sup>87</sup> and the similarity involved 71% of the MAG. Together these results further support the presence of multiple *Psychrobacter* species within the eastern-oyster microbiome. Additional metagenomic sequencing to provide more complete, higher-quality assemblies should help further resolve the relationships between these potentially novel isolates or species and existing *Psychrobacter* isolates and help clarify their potential role(s) in the oyster holobiont.

### Denitrification genes in *Psychrobacter* metagenome assembled genomes and similar RefSeq genomes

The denitrification process is performed by a diverse range of microorganisms, especially under oxygen depleted conditions, with the complete reduction of  $\text{NO}_3^-$  to  $\text{N}_2$  performed via a four-step process, involving the membrane-bound  $\text{NO}_3^-$  reductases (narG) and/or the

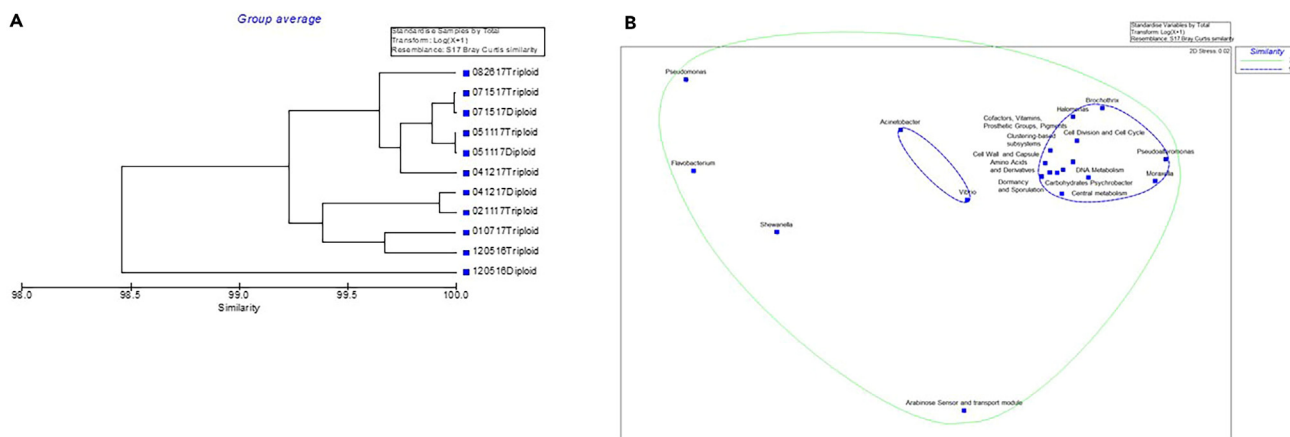


**Figure 6. Statistical correlations between the top 10 bacteria (genus level) and SEED subsystems (level 1) from the eastern oyster metagenomes across ploidy and growth time points**

Shown plotted as a dendrogram analysis are (A), or a Non-metric Multi-Dimensional Scaling plot (NMDS) (B), respectively, where similarity at 75% and 95% is shown.

periplasmic *napA* genes, the  $\text{NO}^{2-}$  reductases NirK (copper-containing) or NirS (containing cytochrome *cd1*) encoded by *nirK* and *nirS*; the NO reductases *cNor* (cytochrome *c* dependent) or *qNor* (quinol-dependent) encoded by *cnor* and *qnor*; and the  $\text{N}_2\text{O}$  reductase *NosZ*.

Sequence-based identification of denitrification genes in the *Psychrobacter* MAGs indicates the presence of *norB* in SPAdes-group-0.8.fa (Table 3). Given the incomplete nature of the MAGs, the search for denitrification genes was extended to the top ANI match for each MAG, under the assumption that the more complete RefSeq genomes would provide a more comprehensive view of the denitrification gene repertoire. This search of the highly similar genomes revealed the presence of *narH* and *narI* for RefSeq genome GCF\_904846635.1 (the top ANI match for SPAdes-group-0.4.fa), and the presence of *narH*, *narI*, *nirK*, and *norB* for RefSeq genome GCF\_904846635.1 (the top ANI match for SPAdes-group-0.8.fa). Other denitrification genes, especially for complete denitrification, such as *nosZ* could not be identified based on the MAG approach. Deeper sequencing depths and coverages will likely enhance our understanding on the metabolic repertoire of *Psychrobacter* spp., associated with eastern oysters.

### Quantitative microbial elemental cycling analysis

When QMEC was used on genomic DNA extracted from homogenized diploid and triploid oysters, a total of 71 genes responsible for CNPS cycling amplified successfully. Note that we did not separate the bacterial biomass from the oyster tissue homogenates, which likely caused PCR inhibition from the overrepresented oyster DNA/mucous and consequently, gene copy abundance/g tissue from only 8 samples covering 3 sampling timepoints yielded usable data (Figures 8A–8D). Regardless, this is the first application of QMEC to understanding biogeochemical cycling in eastern oysters. Relative abundances of CNPS genes were higher in samples collected in December 2016 but did not vary much except in samples collected on April 12, 2017, which seems to be an outlier. PCA conducted on absolute and relative CNPS gene copy numbers revealed differences between diploid and triploid samples but not the sampling time points (Figure 8E and 8F), which was not in line with the taxonomic data-which suggested that season but not ploidy was the stronger of the two factors in structuring oyster microbiomes. However, it may not be prudent to compare shotgun and qPCR data.

**Table 1. Metagenome-assembled genomes (MAG) reconstructed from the eastern oysters in this study are reported in the table**

MAG	Taxonomy (family; genus)	Contig number	Total length bp	BUSCO % complete (single copy, duplicated, fragmented)
SPAdes-group-0.1.fa	<i>Moraxellaceae; Psychrobacter</i>	893	3004744	41.2 (22.6, 8.1, 10.5)
SPAdes-group-0.4.fa	<i>Moraxellaceae; Psychrobacter</i>	474	1479441	38.7 (30.6, 0, 8.1)
SPAdes-group-0.5.fa	<i>Moraxellaceae; Psychrobacter</i>	455	1873903	47.6 (38.7, 0, 8.9)
SPAdes-group-0.7.fa	<i>Alteromonadaceae; Pseudoalteromonas</i>	745	4536590	77.4 (75.8, 0.8, 0.8)
SPAdes-group-0.8.fa	<i>Moraxellaceae; Psychrobacter</i>	665	1695251	25 (16.1, 0, 8.9)
SPAdes-group-0.11.fa	COTS27; _	317	1427112	79.9 (70.2, 0, 9.7)

Metagenome-assembled genomes (MAG) based taxonomy and completeness from the eastern-oyster derived shallow shotgun metagenomic data.

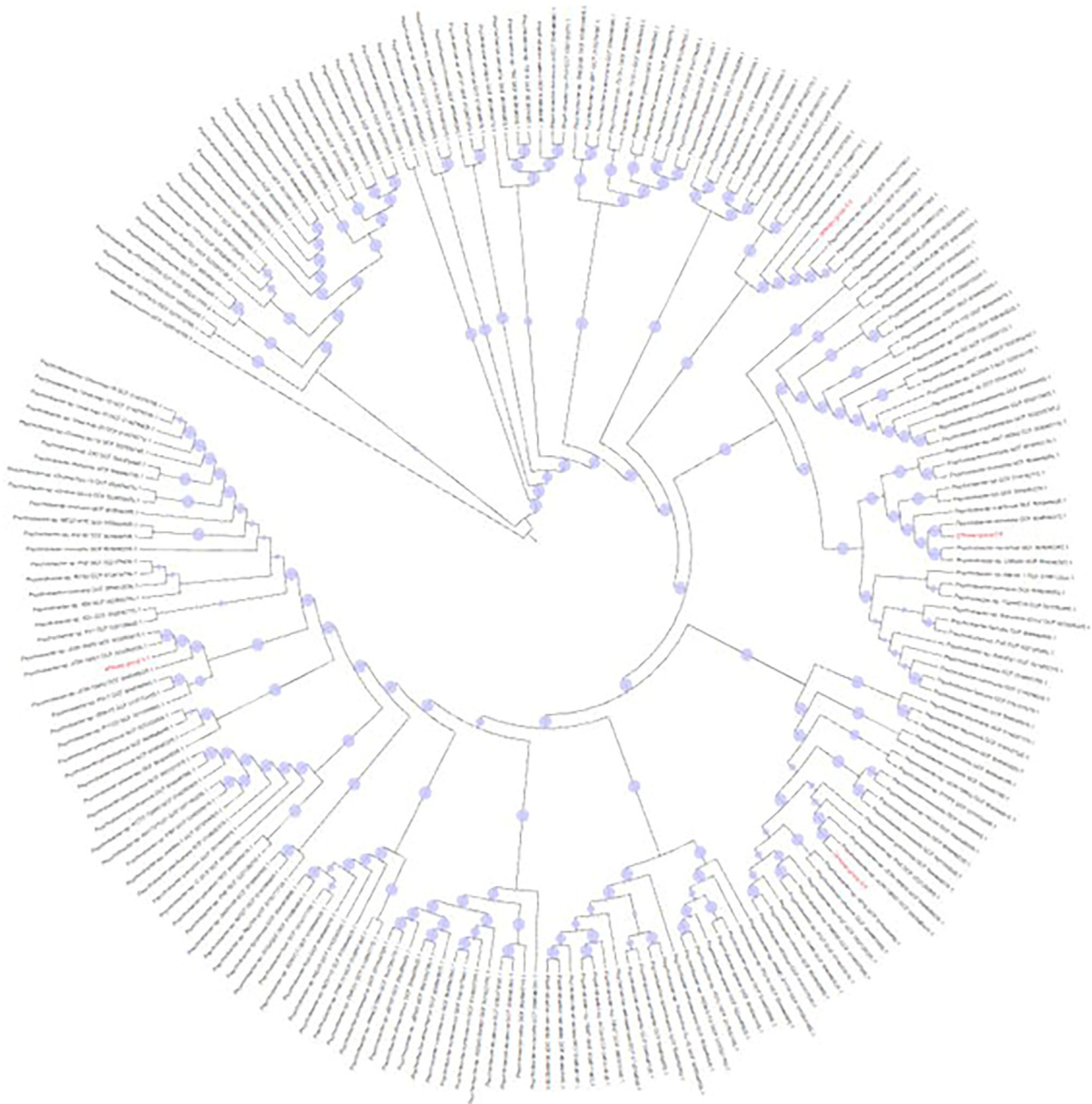


**Figure 7. Maximum likelihood tree of *Psychrobacter* MAG proteomes obtained from this study**

Shown are the *Psychrobacter* MAG proteomes (red labels) relative to RefSeq *Psychrobacter* proteomes from NCBI (black labels). Bootstrap support from 100 replicates is indicated using blue circles.

Among the carbon cycling genes, C-fixation was the most abundant process followed by methane production and oxidation (Figure 9A). Carbon fixation has been found to be an enriched gene function in the mucus microbiomes associated with corals<sup>88</sup> as well as the microbiome of the Black-Lipped Pearl Oyster.<sup>60</sup> *Psychrobacter* spp. were abundant in the coral mucus study, and it is likely that they are important in carbon cycling processes.<sup>88,89</sup> Methane formation (methanogenesis) and oxidation has also been shown to be driven by macrofaunal organisms, such as the bivalve *Limecola balthica* and the polychaete *Marenzelleria arctica*.<sup>90</sup> Furthermore, symbiotic associations between methane-producing archaeal communities and bivalves have also been previously reported<sup>90</sup>; these processes were also identified in the tested eastern oysters, albeit at lower levels. Among the tested 22 nitrogen cycling genes, denitrification was the highest followed by ammonification

**Table 2. Average nucleotide identities (ANI) matches of top MAGs from this study**

MAG	Highest ANI	Percentage of MAG aligned as orthologous matches	RefSeq organism name	RefSeq assembly accession
SPAdes-group-0.1.fa	88.03	70.82	<i>Psychrobacter</i> sp. KH172YL61	GCF_007182895.1
SPAdes-group-0.4.fa	98.32	97.22	<i>Psychrobacter</i> sp. JCM18903	GCF_904846635.1
SPAdes-group-0.5.fa	98.45	97.08	<i>Psychrobacter celer</i>	GCF_904845945.1
SPAdes-group-0.8.fa	96.61	70.58	<i>Psychrobacter maritimus</i>	GCF_904846345.1

Top ANI matches for *Psychrobacter* MAGs reconstructed from the eastern oyster derived shallow shotgun metagenomic data.

(Figure 9B). Note that denitrification in oysters can contribute significantly in N transformations in pelagic regions,<sup>91</sup> as well as in oyster reefs, aquaculture sites, and their sediments.<sup>92–94</sup> In fact, it is the oyster-associated denitrifier microbiota that contribute to cycling reactive N into N<sub>2</sub> gas<sup>9,38</sup> via three pathways: (1) through increasing organic matter deposits in sediments, (2) hosting denitrifying bacteria within gills and/or digestive organs and/or (3) facilitating habitat for other filter-feeding macrofaunal communities.<sup>9</sup> Organic phosphorus (P) mineralization and sulfur (S) oxidation were the major pathways in P and S biogeochemical cycling processes (Figure 9C and 9D).

Among the denitrification genes encoding for nitrite reductase (*nirS* or *nirK*) or nitrous oxide reductase (*nosZ*), *nosZI* was the most dominant (Figure 10A). Under anaerobic conditions, denitrification occurs as a stepwise reduction of nitrate (NO<sub>3</sub><sup>-</sup>) to either nitrous oxide (N<sub>2</sub>O) or dinitrogen gas (N<sub>2</sub>). Complete denitrification takes place via the reduction of nitric oxide (NO) to N<sub>2</sub>O and then the reduction of N<sub>2</sub>O to N<sub>2</sub> gas. The two microbially mediated enzymes facilitating the denitrification process are nitric oxide reductase (NOR) and nitrous oxide reductase (N<sub>2</sub>OR). Based on genotypic studies, *nosZ* gene has been subdivided into clade I (*nosZI*) or clade II (*nosZII*),<sup>95,96</sup> with the latter dominant in most habitats including eastern oysters. Clade I *nosZ* gene containing bacteria mainly belong to Alphaproteobacteria, Betaproteobacteria, and Gammaproteobacteria, but clade II *nosZ* gene has been identified from a variety of bacterial taxa, such as Deltaproteobacteria, Bacteroidetes, and Gemmatimonadetes,<sup>95–97</sup> respectively.

More recently, it was found that autochthonous “core” microbiomes within eastern oysters were significantly ( $p < 0.05$ ) enriched with 933 KEGG based gene functions relative to the 700 gene functions associated with the allochthonous oligotypes.<sup>29</sup> The autochthonous oligotypes were also significantly enriched for several N-cycling genes, such as for dissimilatory nitrate reduction, nitrogen fixation, and nitrification pathways relative to the allochthonous oligotypes. To this end, Arken et al., 2017 showed that an increase in denitrification rates correlated positively to an increase in the gene abundances of *nosZI*, but this trend did not hold for the more dominant *nosZII*. This suggests that oyster-associated microbes possessing the *nosZI* genes may be more significant to denitrification processes than those that possess the *nosZII* genes. However, other reports have shown that *nosZII* denitrifiers are dominant over the *nosZI* denitrifiers in a variety of different ecosystems,<sup>96–98</sup> including the eastern oysters.<sup>38</sup> This could be because the *nosZII* gene renders ecophysiological diversity relative to the *nosZI* gene,<sup>95</sup> suggesting that denitrifier microbiota in oysters are likely far more diverse than previously known. Moreover, in this study, the *nasA*, *narG*, and *napA* genes were also observed (Figure 10B), along with the with dominant *narG* gene. It is known that the *NarG* encodes for membrane-bound nitrate reductase,<sup>99</sup> which has previously been found to be high in sediments from oyster farms<sup>100</sup> and appears to be dominant in eastern oysters, regardless of ploidy. The higher abundances of *nosZII* and *narG*, relative to 16S genes in eastern oysters using the QMEC method are shown in Figure 10C.

In conclusion, overall, this study coupled the use of shallow shotgun metagenomics and high-throughput qPCR (HT-qPCR) to enhance our understanding on the resident “core” or autochthonous microbial communities within the eastern oysters. Regardless of ploidy and season,

**Table 3. Denitrification genes identified in *Psychrobacter* MAGs obtained from this study are shown in the table**

MAG or RefSeq genome	Number of query proteins	Denitrification genes
SPAdes-group-0.1.fa	2452	–
SPAdes-group-0.4.fa	1133	–
SPAdes-group-0.5.fa	1482	–
SPAdes-group-0.8.fa	1429	<i>norB</i> (WP_201628849.1)
GCF_007182895.1	2585	–
GCF_904846635.1	2815	<i>narH</i> (WP_055125087.1), <i>narI</i> (WP_045447153.1)
GCF_904845945.1	2433	–
GCF_904846345.1	2565	<i>narH</i> (WP_201628839.1), <i>narI</i> (WP_201562832.1), <i>nirK</i> (WP_227670896.1), <i>norB</i> (WP_201628849.1)

Shown are the denitrification genes from the *Psychrobacter* MAGs reconstructed from the eastern oyster derived shallow shotgun metagenomic data and similar RefSeq genomes.

<sup>a</sup>The NCBI RefSeq accession of the top BLAST hit in the RefSeq protein database is provided for *norB* in SPAdes-group-0.8.fa. For the other genes in this column the NCBI RefSeq accession is provided for the corresponding protein sequence encoded by the RefSeq genome.

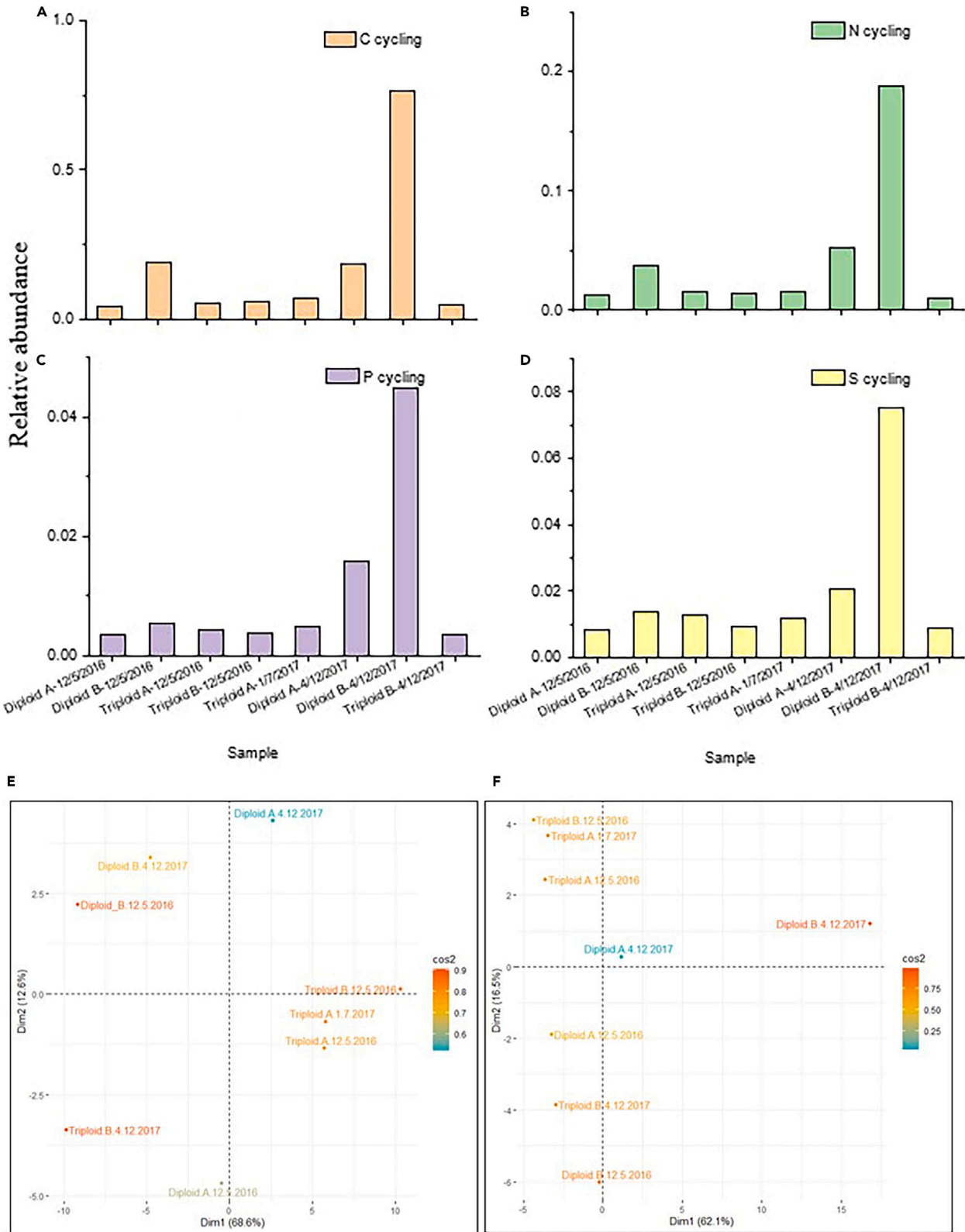


**Figure 8. Quantitative microbial element cycling (QMEC) analysis from the eastern oyster over ploidy and time points**

Shown are A, relative abundance of carbon (C); B, nitrogen (N), C, phosphorus (P) and sulfur (S) cycling genes using QMEC analysis. Also shown are principal component analysis (PCA) of absolute (E) and relative (F) gene copy numbers that indicated ploidy to have a significant impact relative to sampling time points.

the eastern oysters were found to be predominantly colonized by bacteria-the Pseudomonadota phylum and *Psychrobacter* genus. Furthermore, the diversity analysis revealed that the eastern oyster microbiome did not differ on ploidy, but there were significant differences due to the sampling time. It is likely that the *Psychrobacter* genus is representative of the eastern oyster’s “core” microbiome due to the predominance and stable numbers of this psychrotrophic bacteria over an annual growth cycle. We also found strong positive correlations of gene functions associated with central metabolism, DNA metabolism and carbohydrate metabolism with *Psychrobacter* spp. Additionally, the metagenome-assembled genomes (MAGs) also confirmed the presence of multiple *Psychrobacter* genomes harboring denitrification genes - *norB*, *narH*, *narI*, *nirK*, and *norB*, thus providing evidence for this genus to be taxonomically and functionally relevant to the eastern oysters. Further assessment of microbially mediated biogeochemical processes was provided by the application of QMEC technique which revealed predominance of carbon (C) and nitrogen (N) cycling genes relative to the phosphorous and sulfur cycling genes, with no specific trends related to ploidy. Interestingly, the nosZII clade was dominant relative to the nosZI clade, thus indicative that this process is likely responsible for the eastern oyster’s role in depleting dissolved nitrogen via denitrification processes.

**Limitations of the study**

The taxonomic preponderance of the *Psychrobacter* genus in the eastern oysters from this study are largely based on shallow shotgun sequencing and therefore, future studies using deeper sequencing will likely lead to a comprehensive understanding of the eastern oyster’s “core” microbiomes. This will likely pave the way for improving oyster productivity and their ecosystem functions via the manipulation of their autochthonous microbial communities. Further extension of this study should be conducted to delineate whether *Psychrobacter* species are beneficial or detrimental to oyster health and associated ecosystem services, including the biogeochemical cycling of nutrients. Given the central role microbiomes play in oysters and other bivalve species, it is imperative to establish a universally accepted standard in defining the “core”,<sup>21</sup> and by inference, the resident or autochthonous bacterial species for the eastern oysters; studies in this direction are also thus warranted.

**STAR★METHODS**

Detailed methods are provided in the online version of this paper and include the following:

- KEY RESOURCES TABLE
- RESOURCE AVAILABILITY
  - Lead contact
  - Materials availability
  - Data and code availability

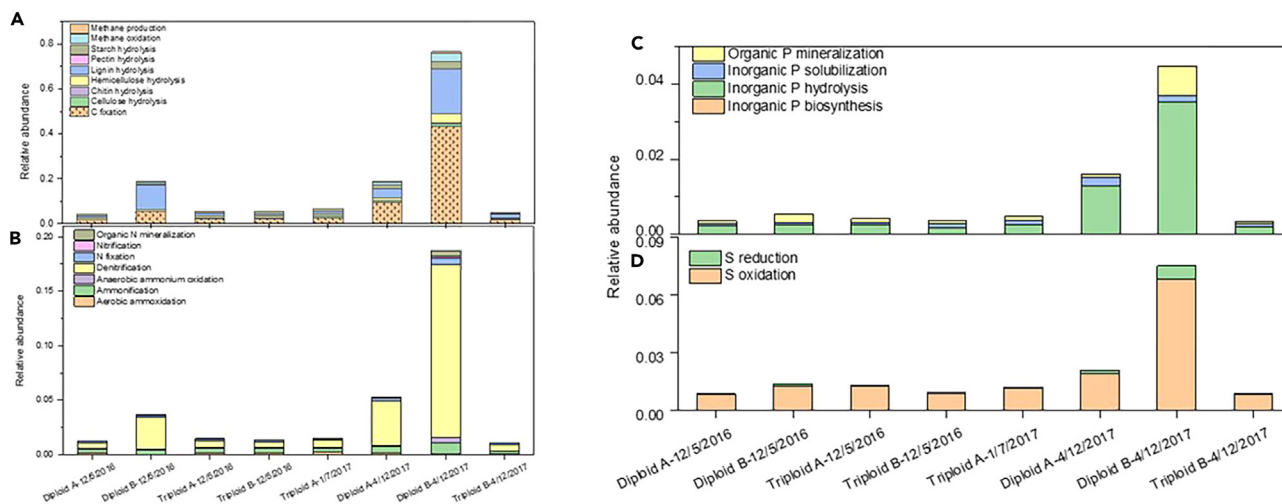


**Figure 9. Major biogeochemical pathways identified in the eastern oyster related to C-fixation, organic phosphorus (P) mineralization and sulfur (S) oxidation**

Shown are A, carbon (C); B, nitrogen (N), C, phosphorus (P) and D, sulfur (S) cycling relative gene abundances when QMEC analysis was performed on the diploid and triploid eastern oysters.

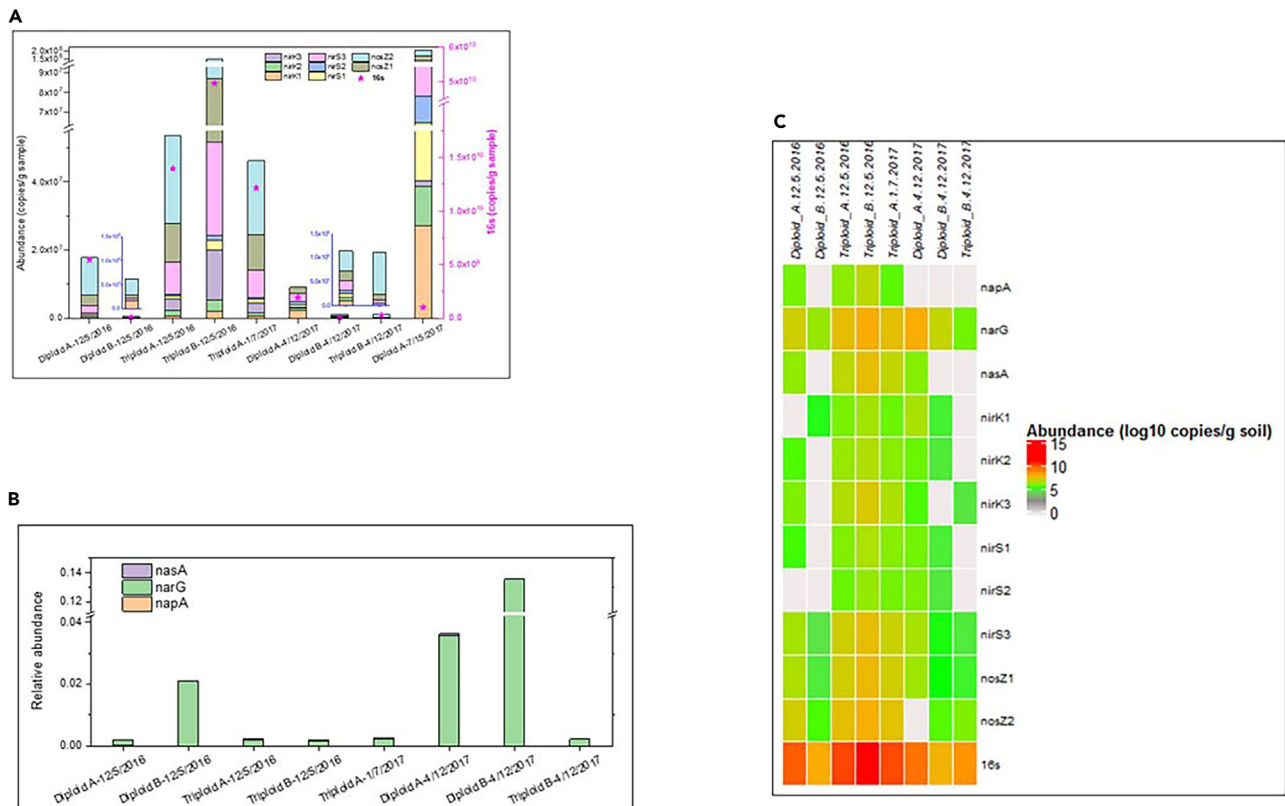


**Figure 10. Major biogeochemical pathways identified in the eastern oyster related to N-cycling**

Shown are copy number of nitrite and nitrate reductase denitrification genes such as (A), nirK, nirS, nosZ; (B) napA, narG, nasA, when QMEC analysis was performed on the diploid and triplod eastern oysters and (C), heatmap of denitrification genes plotted along with the 16S for comparisons.

#### ● METHOD DETAILS AND BIOINFORMATICS

- Sample collection, experimental model, and study participant details
- DNA extraction and library preparation for next-generation sequencing
- DNA sequencing, quality control analysis, data curation, and sequence processing
- High-throughput- quantitative microbial element cycling
- Metagenome assembled genomes
- Phylogenetic analysis of binned metagenomes
- Average nucleotide identity analysis of metagenome assembled genomes
- Identification of denitrification genes in metagenome assembled genomes and RefSeq genomes
- Shallow shotgun metagenome submission: metagenomic sequence accession numbers
- Summary of data transformation
- Statistical analysis

#### SUPPLEMENTAL INFORMATION

Supplemental information can be found online at <https://doi.org/10.1016/j.isci.2024.110193>.

#### ACKNOWLEDGMENTS

This work was mainly supported by a National Science Foundation (NSF) award (#1901371). Other funding also partly supported this research, including Cooperative Agreement NA11SEC4810001 between the National Oceanic and Atmospheric Administration's Educational Partnership Program for Minority Serving Institutions and the Environmental Cooperative Science Center at Florida A&M University, NSF award #2200615 and three US Department of Energy (DOE) projects, that included the Minority Serving Institution Partnership Program (MSIPP) (task order agreements #0000403081, #0000403082, and #0000456318). We thank B. Ballard and A. Wynn from the Wakulla Environmental Institute for supplying oysters and assisting with field collections. We also appreciate Deborah Keller and Erich Martin for providing photos

of our study site located in Florida. Technical help provided by Drs. Meenakshi Agarwal, Rajneesh Jaswal, and Rajesh S. Rathore is also much appreciated.

## AUTHOR CONTRIBUTIONS

AC, AP, CHJ, and MM contributed to conception and design of the study. AP organized the database and performed the statistical analysis. AP wrote the first draft of the article. AC, AP, MM, PS, JQS, YZ, XYZ, CC, and CHJ wrote sections of the article. All authors contributed to article revision, read, and approved the submitted version.

## DECLARATION OF INTERESTS

The authors declare that the research was conducted in the absence of any commercial or financial relationships that could be construed as a potential conflict of interest.

Received: December 29, 2023

Revised: April 9, 2024

Accepted: June 3, 2024

Published: June 6, 2024

## REFERENCES

1. Cruz-Romero, M.C., Kerry, J.P., and Kelly, A.L. (2008). Fatty acids, volatile compounds and colour changes in high-pressure-treated oysters (*Crassostrea gigas*). *Innov. Food Sci. Emerg. Technol.* 9, 54–61. <https://doi.org/10.1016/j.ifset.2007.05.003>.
2. Chen, H., Wang, M., Yang, C., Wan, X., Ding, H.H., Shi, Y., and Zhao, C. (2019). Bacterial spoilage profiles in the gills of Pacific oysters (*Crassostrea gigas*) and Eastern oysters (*C. virginica*) during refrigerated storage. *Food Microbiol.* 82, 209–217. <https://doi.org/10.1016/j.fm.2019.02.008>.
3. (2020). National Marine Fisheries Service. [https://www.st.nmfs.noaa.gov/st1/commercial/landings/annual\\_landings.html](https://www.st.nmfs.noaa.gov/st1/commercial/landings/annual_landings.html).
4. Fisheries and Agriculture Organisation of the United Nations [FAO] (2018). *The State of World Fisheries and Aquaculture 2018. Meeting the Sustainable Development Goals (FAO)*. <https://www.fao.org/family-farming/detail/en/c/1145050>.
5. Prapaiwong, N., Wallace, R.K., and Arias, C.R. (2009). Bacterial loads and microbial composition in high pressure treated oysters during storage. *Int. J. Food Microbiol.* 131, 145–150. <https://doi.org/10.1016/j.ijfoodmicro.2009.02.014>.
6. Burge, C.A., Mark Eakin, C., Friedman, C.S., Froelich, B., Hershberger, P.K., Hofmann, E.E., Petes, L.E., Prager, K.C., Weil, E., Willis, B.L., et al. (2014). Climate change influences on marine infectious diseases: implications for management and society. *Ann. Rev. Mar. Sci.* 6, 249–277. <https://doi.org/10.1146/annurev-marine-010213-135029>.
7. Chesapeake Bay Foundation (2003). *Oyster Facts Sheet*. <https://www.cbf.org/about-the-bay/chesapeake-wildlife/eastern-oysters/oyster-fact-sheet.html>.
8. Bricker, S.B., Grizzle, R.E., Trowbridge, P., Rose, J.M., Ferreira, J.G., Wellman, K., Zhu, C., Galimany, E., Wikfors, G.H., Saurel, C., et al. (2020). Bioextractive Removal of Nitrogen by Oysters in Great Bay Piscataqua River Estuary, New Hampshire, USA. *Estuaries Coast.* 43, 23–38. <https://doi.org/10.1007/s12237-019-00661-8>.
9. Ayvazian, S., Mulvaney, K., Zarnoch, C., Palta, M., Reichert-Nguyen, J., McNally, S., Pilaro, M., Jones, A., Terry, C., and Fulweiler, R.W. (2021). Beyond Bioextraction: The Role of Oyster-Mediated Denitrification in Nutrient Management. *Environ. Sci. Technol.* 55, 14457–14465. <https://doi.org/10.1021/acs.est.1c01901>.
10. Filippini, G., Dafforn, K.A., and Bugnot, A.B. (2023). Shellfish as a bioremediation tool: A review and meta-analysis. *Environ. Pollut.* 316, 120614. <https://doi.org/10.1016/j.envpol.2022.120614>.
11. Wilberg, M.J., Livings, M.E., Barkman, J.S., Morris, B.T., and Robinson, J.M. (2011). Overfishing, disease, habitat loss, and potential extirpation of oysters in upper Chesapeake Bay. *Mar. Ecol. Prog. Ser.* 436, 131–144. <https://doi.org/10.3354/meps09161>.
12. Hemraj, D.A., Bishop, M.J., Hancock, B., Minuti, J.J., Thurstan, R.H., Zu Ermgassen, P.S.E., and Russell, B.D. (2022). Oyster reef restoration fails to recoup global historic ecosystem losses despite substantial biodiversity gain. *Sci. Adv.* 8, eabp8747. <https://doi.org/10.1126/sciadv.abp8747>.
13. Kirby, M.X. (2004). Fishing down the coast: Historical expansion and collapse of oyster fisheries along continental margins. *Proc. Natl. Acad. Sci. USA* 101, 13096–13099. <https://doi.org/10.1073/pnas.0405150101>.
14. Qin, Y., Zhang, Y., Mo, R., Zhang, Y., Li, J., Zhou, Y., Ma, H., Xiao, S., and Yu, Z. (2019). Influence of ploidy and environment on grow-out traits of diploid and triploid Hong Kong oysters *Crassostrea hongkongensis* in southern China. *Aquaculture* 507, 108–118. <https://doi.org/10.1016/j.aquaculture.2019.04.017>.
15. Bodenstern, S., Callam, B.R., Walton, W.C., Rikard, F.S., Tiersch, T.R., and La Peyre, J.F. (2023). Survival and growth of triploid eastern oysters, *Crassostrea virginica*, produced from wild diploids collected from low-salinity areas. *Aquaculture* 564, 739032. <https://doi.org/10.1016/j.aquaculture.2022.739032>.
16. Hollier, D. (2014). Tasty Mutants: The Invention of the Modern Oyster. In: *Atl.* <https://www.theatlantic.com/technology/archive/2014/09/todays-oysters-are-mutants/380858/>.
17. Gagnaire, B., Soletchnik, P., Madec, P., Geairon, P., Le Moine, O., and Renault, T. (2006). Diploid and triploid Pacific oysters, *Crassostrea gigas* (Thunberg), reared at two heights above sediment in Marennes-Oleron Basin, France: Difference in mortality, sexual maturation and hemocyte parameters. *Aquaculture* 254, 606–616. <https://doi.org/10.1016/j.aquaculture.2005.10.008>.
18. Unzueta-Martínez, A., Welch, H., and Bowen, J.L. (2022). Determining the Composition of Resident and Transient Members of the Oyster Microbiome. *Front. Microbiol.* 12, 828692. <https://doi.org/10.3389/fmicb.2021.828692>.
19. Romero, J., García-Varela, M., Lacleste, J.P., and Espejo, R.T. (2002). Bacterial 16S rRNA gene analysis revealed that bacteria related to *Arcobacter* spp. constitute an abundant and common component of the oyster microbiota (*Tiostrea chilensis*). *Microb. Ecol.* 44, 365–371. <https://doi.org/10.1007/s00248-002-1063-7>.
20. Lokmer, A., Goedknecht, M.A., Thielges, D.W., Fiorentino, D., Kuenzel, S., Baines, J.F., and Wegner, K.M. (2016). Spatial and Temporal Dynamics of Pacific Oyster Hemolymph Microbiota across Multiple Scales. *Front. Microbiol.* 7, 1367. <https://doi.org/10.3389/fmicb.2016.01367>.
21. Shade, A., and Handelsman, J. (2012). Beyond the Venn diagram: the hunt for a core microbiome. *Environ. Microbiol.* 14, 4–12. <https://doi.org/10.1111/j.1462-2920.2011.02585.x>.
22. De Decker, S., Normand, J., Saulnier, D., Pernet, F., Castagnet, S., and Boudry, P. (2011). Responses of diploid and triploid Pacific oysters *Crassostrea gigas* to *Vibrio* infection in relation to their reproductive status. *J. Invertebr. Pathol.* 106, 179–191. <https://doi.org/10.1016/j.jip.2010.09.003>.
23. Colwell, R.R., and Liston, J. (1960). Microbiology of shellfish. Bacteriological study of the natural flora of Pacific oysters (*Crassostrea gigas*). *Appl. Microbiol.* 8, 104–109. <https://doi.org/10.1128/am.8.2.104-109.1960>.
24. Zurel, D., Benayahu, Y., Or, A., Kovacs, A., and Gophna, U. (2011). Composition and dynamics of the gill microbiota of an invasive Indo-Pacific oyster in the eastern Mediterranean Sea. *Environ. Microbiol.* 13,



- 1467–1476. <https://doi.org/10.1111/j.1462-2920.2011.02448.x>.
25. Trabal Fernández, N., Mazón-Suástegui, J.M., Vázquez-Juárez, R., Ascencio-Valle, F., and Romero, J. (2014). Changes in the composition and diversity of the bacterial microbiota associated with oysters (*Crassostrea corteziensis*, *Crassostrea gigas* and *Crassostrea sikamea*) during commercial production. *FEMS Microbiol. Ecol.* 88, 69–83. <https://doi.org/10.1111/1574-6941.12270>.
  26. Prieur, D., Mevel, G., Nicolas, J.L., Plusquellec, A., and Vigneulle, M. (1990). Interactions between bivalve molluscs and bacteria in the marine environment. *Oceanogr. Mar. Biol. Annu. Rev.* 28, 277–352.
  27. Newton, I.L.G., Woyke, T., Auchtung, T.A., Dilly, G.F., Dutton, R.J., Fisher, M.C., Fontanez, K.M., Lau, E., Stewart, F.J., Richardson, P.M., et al. (2007). The *Calypotoga magna* chemoautotrophic symbiont genome. *Science* 315, 998–1000. <https://doi.org/10.1126/science.1138438>.
  28. Pujalte, M.J., Ortigosa, M., Macián, M.C., and Garay, E. (1999). Aerobic and facultative anaerobic heterotrophic bacteria associated to Mediterranean oysters and seawater. *Int. Microbiol.* 2, 259–266.
  29. Sakowski, E.G., Wommack, K.E., and Polson, S.W. (2020). Oyster Calcifying Fluid Harbors Persistent and Dynamic Autochthonous Bacterial Populations That May Aid in Shell Formation. *Mar. Ecol. Prog. Ser.* 653, 57–75. <https://doi.org/10.3354/meps13487>.
  30. Banker, R., and Vermeij, G.J. (2018). Oyster microbial communities and implications for chalk deposit formation. *Hydrobiologia* 816, 121–135. <https://doi.org/10.1007/s10750-018-3569-0>.
  31. Braissant, O., Decho, A.W., Dupraz, C., Glunk, C., Przekop, K.M., and Visscher, P.T. (2007). Exopolymeric substances of sulfate-reducing bacteria: Interactions with calcium at alkaline pH and implication for formation of carbonate minerals. *Geobiology* 5, 401–411. <https://doi.org/10.1111/j.1472-4669.2007.00117.x>.
  32. Cacchio, P., Ercole, C., Contento, R., Cappuccio, G., Preite Martinez, M., Del Gallo, M., and Lepidi, A. (2012). Involvement of bacteria in the origin of a newly described speleothem in the gypsum cave of grave grubbo (Crotona, Italy). *J. Cave Karst Stud.* 74, 7–18. <https://doi.org/10.4311/2010MB0136R>.
  33. Hines, I.S., Markov Madanick, J., Smith, S.A., Kuhn, D.D., and Stevens, A.M. (2023). Analysis of the core bacterial community associated with consumer-ready Eastern oysters (*Crassostrea virginica*). *PLoS One* 18, e0281747. <https://doi.org/10.1371/journal.pone.0281747>.
  34. Akter, S., Wos-Oxley, M.L., Catalano, S.R., Hassan, M.M., Li, X., Qin, J.G., and Oxley, A.P. (2023). Host Species and Environment Shape the Gut Microbiota of Cohabiting Marine Bivalves. *Microb. Ecol.* 86, 1755–1772. <https://doi.org/10.1007/s00248-023-02192-z>.
  35. Singh, P., Williams, D., Velez, F.J., and Nagpal, R. (2022). Comparison of the Gill Microbiome of Retail Oysters from Two Geographical Locations Exhibited Distinct Microbial Signatures: A Pilot Study for Potential Future Applications for Monitoring Authenticity of Their Origins. *Appl. Microbiol.* 3, 1–10.
  36. Pierce, M.L., and Ward, J.E. (2019). Gut Microbiomes of the Eastern Oyster (*Crassostrea virginica*) and the Blue Mussel (*Mytilus edulis*): Temporal Variation and the Influence of Marine Aggregate-Associated Microbial Communities. *mSphere* 4, e00730-19. <https://doi.org/10.1128/mSphere.00730-19>.
  37. King, G.M., Judd, C., Kuske, C.R., and Smith, C. (2012). Analysis of stomach and gut microbiomes of the eastern oyster (*Crassostrea virginica*) from coastal Louisiana, USA. *PLoS One* 7, e51475. <https://doi.org/10.1371/journal.pone.0051475>.
  38. Arfken, A., Song, B., Bowman, J.S., and Piehler, M. (2017). Denitrification potential of the eastern oyster microbiome using a 16S rRNA gene based metabolic inference approach. *PLoS One* 12, e0185071. <https://doi.org/10.1371/journal.pone.0185071>.
  39. Stevick, R.J., Sohn, S., Modak, T.H., Nelson, D.R., Rowley, D.C., Tammi, K., Smolowitz, R., Markey Lundgren, K., Post, A.F., and Gómez-Chiari, M. (2019). Bacterial Community Dynamics in an Oyster Hatchery in Response to Probiotic Treatment. *Front. Microbiol.* 10, 1060. <https://doi.org/10.3389/fmicb.2019.01060>.
  40. Pimentel, Z.T., Keith, D.-T., T.R.K., et al. (2021). Microbiome Analysis Reveals Diversity and Function of Molluscs Associated with the Eastern Oyster, *Crassostrea virginica*. *mSphere* 6, e00227-21. <https://doi.org/10.1128/mSphere.00227-21>.
  41. Banker, R.M.W., and Coil, D. (2020). Inoculation With *Desulfovibrio* sp. Does Not Enhance Chalk Formation in the Pacific Oyster. *Front. Mar. Sci.* 7. <https://doi.org/10.3389/fmars.2020.00407>.
  42. Britt, A., Bernini, M., McSweeney, B., Dalapati, S., Duchin, S., Cavanna, K., Santos, N., Donovan, G., O'Byrne, K., Noyes, S., et al. (2020). The effects of atrazine on the microbiome of the eastern oyster: *Crassostrea virginica*. *Sci. Rep.* 10, 11088. <https://doi.org/10.1038/s41598-020-67851-4>.
  43. Chauhan, A., Wafula, D., Lewis, D.E., and Pathak, A. (2014). Metagenomic assessment of the eastern oyster-associated microbiota. *Genome Announc.* 2, e01083-14. <https://doi.org/10.1128/genomeA.01083-14>.
  44. Thomas, J.C., 4th, Wafula, D., Chauhan, A., Green, S.J., Gragg, R., and Jagoe, C. (2014). A survey of deepwater horizon (DWH) oil-degrading bacteria from the Eastern oyster biome and its surrounding environment. *Front. Microbiol.* 5, 149. <https://doi.org/10.3389/fmicb.2014.00149>.
  45. Pathak, A., Stothard, P., and Chauhan, A. (2021). Comparative Genomic Analysis of Three *Pseudomonas* Species Isolated from the Eastern Oyster (*Crassostrea virginica*) Tissues, Mantle Fluid, and the Overlying Estuarine Water Column. *Microorganisms* 9, 490. <https://doi.org/10.3390/microorganisms9030490>.
  46. Chauhan, A., Green, S., Pathak, A., Thomas, J., and Venkatraman, R. (2013). Whole-genome sequences of five oyster-associated bacteria show potential for crude oil hydrocarbon degradation. *Genome Announc.* 1, e00802-13. <https://doi.org/10.1128/genomeA.00802-13>.
  47. Vitousek, P.M., Aber, J.D., Howarth, R.W., Likens, G.E., Matson, P.A., Schindler, D.W., Schlesinger, W.H., and Tilman, D.G. (1997). Human alteration of the global nitrogen cycle: sources and consequences. *Ecol. Appl.* 7, 737–750.
  48. Ray, N.E., Hancock, B., Brush, M.J., Colden, A., Cornwell, J., Labrie, M.S., Maguire, T.J., Maxwell, T., Rogers, D., Stevick, R.J., et al. (2021). A review of how we assess denitrification in oyster habitats and proposed guidelines for future studies. *Limnol. Oceanogr. Methods* 19, 714–731. <https://doi.org/10.1002/lom3.10456>.
  49. Zumft, W.G. (1997). Cell biology and molecular basis of denitrification. *Microbiol. Mol. Biol. Rev.* 61, 533–616. <https://doi.org/10.1128/mmlr.61.4.533-616.1997>.
  50. Lugli, G.A., and Ventura, M. (2022). A breath of fresh air in microbiome science: shallow shotgun metagenomics for a reliable disentangling of microbial ecosystems. *Microbiome Res. Rep.* 1, 8. <https://doi.org/10.20517/mrr.2021.07>.
  51. Zheng, B., Zhu, Y., Sardans, J., Peñuelas, J., and Su, J. (2018). QMEC: a tool for high-throughput quantitative assessment of microbial functional potential in C, N, P, and S biogeochemical cycling. *Sci. China Life Sci.* 61, 1451–1462. <https://doi.org/10.1007/s11427-018-9364-7>.
  52. Kobiyama, A., Ikeo, K., Reza, M.S., Rashid, J., Yamada, Y., Ikeda, Y., Ikeda, D., Mizusawa, N., Sato, S., Ogata, T., et al. (2018). Metagenome-based diversity analyses suggest a strong locality signal for bacterial communities associated with oyster aquaculture farms in Ofunato Bay. *Gene* 665, 149–154. <https://doi.org/10.1016/j.gene.2018.04.073>.
  53. Yu, M., Wang, X., and Yan, A. (2021). Microbial Profiles of Retail Pacific Oysters (*Crassostrea gigas*) from Guangdong Province, China. *Front. Microbiol.* 12, 689520. <https://doi.org/10.3389/fmicb.2021.689520>.
  54. Li, S., Young, T., Archer, S., Lee, K., Sharma, S., and Alfaro, A.C. (2022). Mapping the Green-Lipped Mussel (*Perna canaliculus*) Microbiome: A Multi-Tissue Analysis of Bacterial and Fungal Diversity. *Curr. Microbiol.* 79, 76. <https://doi.org/10.1007/s00284-021-02758-5>.
  55. Kamiyama, T., Yamauchi, H., Iwai, T., and Hamasaki, K. (2009). Seasonal variations in abundance and biomass of picoplankton in an oyster-farming area of northern Japan. *Plankt. Benthos Res.* 4, 62–71. <https://doi.org/10.3800/pbr.4.62>.
  56. Natrah, F.M.I., Bossier, P., Sorgeloos, P., Yusoff, F.M., and Defoirdt, T. (2014). Significance of microalgal–bacterial interactions for aquaculture. *Rev. Aquac.* 6, 48–61. <https://doi.org/10.1111/raq.12024>.
  57. Hernández-Zárate, G., and Olmos-Soto, J. (2006). Identification of bacterial diversity in the oyster *Crassostrea gigas* by fluorescent in situ hybridization and polymerase chain reaction. *J. Appl. Microbiol.* 100, 664–672.
  58. Rappé, M.S., Vergin, K., and Giovannoni, S.J. (2000). Phylogenetic comparisons of a coastal bacterioplankton community with its counterparts in open ocean and freshwater systems. *FEMS Microbiol. Ecol.* 33, 219–232. <https://doi.org/10.1111/j.1574-6941.2000.tb00744.x>.
  59. Kersters, K., De Vos, P., Gillis, M., et al. (2006). In Introduction to the Proteobacteria BT - The Prokaryotes: Volume 5: Proteobacteria: Alpha and Beta Subclasses, M. Dworkin, S. Falkow, and E. Rosenberg, et al., eds. (Springer), pp. 3–37.

60. Dubé, C.E., Ky, C.L., and Planes, S. (2019). Microbiome of the Black-Lipped Pearl Oyster *Pinctada margaritifera*, a Multi-Tissue Description With Functional Profiling. *Front. Microbiol.* 10, 1548. <https://doi.org/10.3389/fmicb.2019.01548>.
61. Pierce, M.L., and Ward, J.E. (2018). Microbial Ecology of the Bivalvia, with an Emphasis on the Family Ostreidae. *J. Shellfish Res.* 37, 793–806. <https://doi.org/10.2983/035.037.0410>.
62. Worden, P.J., Bogema, D.R., Micallef, M.L., Jeffrey, G., Deutscher, A.T., Labbate, M., Green, T.J., King, W.L., Liu, M., Seymour, J.R., and Jenkins, C. (2022). Phylogenomic diversity of *Vibrio* species and other Gammaproteobacteria isolated from Pacific oysters (*Crassostrea gigas*) during a summer mortality outbreak. *Microb. Genom.* 8, 000883. <https://doi.org/10.1099/mgen.0.000883>.
63. Zeng, Y.-X., Yu, Y., Liu, Y., and Li, H.-R. (2016). *Psychrobacter glaciei* sp. nov., isolated from the ice core of an Arctic glacier. *Int. J. Syst. Evol. Microbiol.* 66, 1792–1798. <https://doi.org/10.1099/ijsem.0.000939>.
64. Bowman, J.P., Nichols, D.S., and McMeekin, T.A. (1997). *Psychrobacter glacincola* sp. nov., a halotolerant, psychrophilic bacterium isolated from Antarctic sea ice. *Syst. Appl. Microbiol.* 20, 209–215. [https://doi.org/10.1016/S0723-2020\(97\)80067-](https://doi.org/10.1016/S0723-2020(97)80067-)
65. Bakermans, C., Ayala-del-Río, H.L., Ponder, M.A., Vishnivetskaya, T., Gilichinsky, D., Thomashow, M.F., and Tiedje, J.M. (2006). *Psychrobacter cryohalolentis* sp. nov. and *Psychrobacter arcticus* sp. nov., isolated from Siberian permafrost. *Int. J. Syst. Evol. Microbiol.* 56, 1285–1291. <https://doi.org/10.1099/ijms.0.64043-0>.
66. Welter, D.K., Ruaud, A., Henseler, Z.M., De Jong, H.N., van Coeverden de Groot, P., Michaux, J., Gormezano, L., Waters, J.L., Youngblut, N.D., and Ley, R.E. (2021). Free-Living, Psychrotrophic Bacteria of the Genus *Psychrobacter* Are Descendants of Pathobionts. *mSystems* 6, e00258-21. <https://doi.org/10.1128/mSystems.00258-21>.
67. Apprill, A., Miller, C.A., Moore, M.J., Durban, J.W., Fearbach, H., and Barrett-Lennard, L.G. (2017). Extensive core microbiome in drone-captured whale blow supports a framework for health monitoring. *mSystems* 2, e00119-17. <https://doi.org/10.1128/mSystems.00119-17>.
68. Kämpfer, P., Glaeser, S.P., Irgang, R., Fernández-Negrete, G., Poblete-Morales, M., Fuentes-Messina, D., Cortez-San Martín, M., and Avendaño-Herrera, R. (2020). *Psychrobacter pygoscelis* sp. nov. isolated from the penguin *Pygoscelis papua*. *Int. J. Syst. Evol. Microbiol.* 70, 211–219. <https://doi.org/10.1099/ijsem.0.003739>.
69. Bakermans, C. (2018). Adaptations to marine versus terrestrial low temperature environments as revealed by comparative genomic analyses of the genus *Psychrobacter*. *FEMS Microbiol. Ecol.* 94. <https://doi.org/10.1093/femsec/fiy102>.
70. Madigan, T.L., Bott, N.J., Torok, V.A., Percy, N.J., Carragher, J.F., de Barros Lopes, M.A., and Kiermeier, A. (2014). A microbial spoilage profile of half shell Pacific oysters (*Crassostrea gigas*) and Sydney rock oysters (*Saccostrea glomerata*). *Food Microbiol.* 38, 219–227. <https://doi.org/10.1016/j.fm.2013.09.005>.
71. Franco, R., Arenal, A., Martín, L., Martínez, Y., Santiesteban, D., Sotolongo, J., Pimentel, E., Carrillo, O., and Bossier, P. (2016). *Psychrobacter* sp. 17-1 enhances growth and survival in early postlarvae of white shrimp, *Penaeus vannamei* Boone, 1931 (Decapoda, Penaeidae). *Crustaceana* 89, 1467–1484. <https://doi.org/10.1163/15685403-00003595>.
72. Caipang, C.M.A., Suharman, I., Avillanosa, A.L., and Bargoyo, V.T. (2020). Host-derived Probiotics for Finfish Aquaculture. *IOP Conf. Ser. Earth Environ. Sci.* 430, 012026. <https://doi.org/10.1088/1755-1315/430/1/012026>.
73. Makled, S.O., Hamdan, A.M., El-Sayed, A.F.M., and Hafez, E.E. (2017). Evaluation of marine psychrophile, *Psychrobacter namhaensis* SO89, as a probiotic in Nile tilapia (*Oreochromis niloticus*) diets. *Fish Shellfish Immunol.* 61, 194–200. <https://doi.org/10.1016/j.fsi.2017.01.001>.
74. Ramírez, C., Rojas, R., and Romero, J. (2020). Partial Evaluation of Autochthonous Probiotic Potential of the Gut Microbiota of *Seriola lalandi*. *Probiotics Antimicrob. Proteins* 12, 672–682. <https://doi.org/10.1007/s12602-019-09550-9>.
75. Tokarsky, O., Marshall, D.L., Dillon, J., and Andrews, L.S. (2019). Long-Term Depuration of *Crassostrea virginica* Oysters at Different Salinities and Temperatures Changes *Vibrio vulnificus* Counts and Microbiological Profile. *J. Food Prot.* 82, 22–29. <https://doi.org/10.4315/0362-028X.JFP-18-225>.
76. Deschaght, P., Janssens, M., Vaneechoutte, M., and Wauters, G. (2012). *Psychrobacter* isolates of human origin, other than *Psychrobacter phenylpyruvicus*, are predominantly *Psychrobacter faecalis* and *Psychrobacter pulmonis*, with emended description of *P. faecalis*. *Int. J. Syst. Evol. Microbiol.* 62, 671–674. <https://doi.org/10.1099/ijms.0.032631-0>.
77. Wirth, S.E., Ayala-del-Río, H.L., Cole, J.A., Kohlerschmidt, D.J., Musser, K.A., Sepúlveda-Torres, L.D.C., Thompson, L.M., and Wolfgang, W.J. (2012). *Psychrobacter sanguinis* sp. nov., recovered from four clinical specimens over a 4-year period. *Int. J. Syst. Evol. Microbiol.* 62, 49–54. <https://doi.org/10.1099/ijms.0.029058-0>.
78. Speights, C.J., Silliman, B.R., and McCoy, M.W. (2017). The effects of elevated temperature and dissolved pCO<sub>2</sub> on a marine foundation species. *Ecol. Evol.* 7, 3808–3814. <https://doi.org/10.1002/ece3.2969>.
79. Li, Y. (2009). Oysters and the impacts of climate change - Responsible Seafood Advocate. <https://www.globalseafood.org>.
80. Avila-Poveda, O.H., Torres-Ariño, A., Girón-Cruz, D.A., and Cuevas-Aguirre, A. (2014). Evidence for accumulation of *Synechococcus elongatus* (Cyanobacteria: Cyanophyceae) in the tissues of the oyster *Crassostrea gigas* (Mollusca: Bivalvia). *Tissue Cell* 46, 379–387. <https://doi.org/10.1016/j.tice.2014.07.001>.
81. Chen, H., Liu, Z., Wang, M., Chen, S., and Chen, T. (2013). Characterisation of the spoilage bacterial microbiota in oyster gills during storage at different temperatures. *J. Sci. Food Agric.* 93, 3748–3754. <https://doi.org/10.1002/jsfa.6237>.
82. Pathak, A., Rathore, R.S., and Chauhan, A. (2022). Comparative Genomic Analysis of Three *Pseudomonas* Species Isolated from the Eastern Oyster (*Crassostrea virginica*). In *Prime Archives in Microbiology, 3rd Edition*, A.M. Albasha, ed. (Vide Leaf).
83. Abreu, C.I., Dal Bello, M., Bunse, C., Pinhasi, J., and Gore, J. (2023). Warmer temperatures favor slower-growing bacteria in natural marine communities. *Sci. Adv.* 9, eade8352. <https://doi.org/10.1126/sciadv.ade8352>.
84. Benhaïm, D., Leblanc, C.A., Horri, K., Mannion, K., Galloway, M., Leeper, A., Knobloch, S., Sigurgeirsson, O., and Thorarensen, H. (2020). The effect of triploidy on the performance, gut microbiome and behaviour of juvenile Atlantic salmon (*Salmo salar*) raised at low temperature. *Appl. Anim. Behav. Sci.* 229, 105031. <https://doi.org/10.1016/j.applanim.2020.105031>.
85. Cantas, L., Fraser, T.W.K., Fjellidal, P.G., Mayer, I., and Sørum, H. (2011). The culturable intestinal microbiota of triploid and diploid juvenile Atlantic salmon (*Salmo salar*) - a comparison of composition and drug resistance. *BMC Vet. Res.* 7, 71. <https://doi.org/10.1186/1746-6148-7-71>.
86. Wada, N., Yuasa, H., Kajitani, R., Gotoh, Y., Ogura, Y., Yoshimura, D., Toyoda, A., Tang, S.L., Higashimura, Y., Sweatman, H., et al. (2020). A ubiquitous subcuticular bacterial symbiont of a coral predator, the crown-of-thorns starfish, in the Indo-Pacific. *Microbiome* 8, 123. <https://doi.org/10.1186/s40168-020-00880-3>.
87. Jain, C., Rodriguez-R, L.M., Phillippy, A.M., Konstantinidis, K.T., and Aluru, S. (2018). High throughput ANI analysis of 90K prokaryotic genomes reveals clear species boundaries. *Nat. Commun.* 9, 5114. <https://doi.org/10.1038/s41467-018-07641-9>.
88. Badhai, J., Ghosh, T.S., and Das, S.K. (2016). Composition and Functional Characterization of Microbiome Associated with Mucus of the Coral Fungia echinata Collected from Andaman Sea. *Front. Microbiol.* 7, 936. <https://doi.org/10.3389/fmicb.2016.00936>.
89. McKew, B.A., Dumbrell, A.J., Daud, S.D., Hepburn, L., Thorpe, E., Mogensen, L., and Whitby, C. (2012). Characterization of geographically distinct bacterial communities associated with coral mucus produced by *Acropora* spp. and *Porites* spp. *Appl. Environ. Microbiol.* 78, 5229–5237. <https://doi.org/10.1128/AEM.07764-11>.
90. Bonaglia, S., Brüchert, V., Callac, N., Vicenzi, A., Chi Fru, E., and Nascimento, F.J.A. (2017). Methane fluxes from coastal sediments are enhanced by macrofauna. *Sci. Rep.* 7, 13145. <https://doi.org/10.1038/s41598-017-13263-w>.
91. Jiang, H., Lan, W., Li, T., Xu, Z., Liu, W., and Pan, K. (2020). Isotopic Composition Reveals the Impact of Oyster Aquaculture on Pelagic Nitrogen Cycling in a Subtropical Estuary. *Water Res.* 187, 116431. <https://doi.org/10.1016/j.watres.2020.116431>.
92. Hoellein, T.J., Zarnoch, C.B., and Grizzle, R.E. (2015). Eastern oyster (*Crassostrea virginica*) filtration, biodeposition, and sediment nitrogen cycling at two oyster reefs with contrasting water quality in Great Bay Estuary (New Hampshire, USA). *Biogeochemistry* 122, 113–129. <https://doi.org/10.1007/s10533-014-0034-7>.
93. Mortazavi, B., Ortmann, A.C., Wang, L., Bernard, R.J., Staudhammer, C.L., Dalrymple, J.D., Carmichael, R.H., and Kleinhuizen, A.A. (2015). Evaluating the impact of oyster (<i>Crassostrea virginica</i>

- l>) gardening on sediment nitrogen cycling in a subtropical estuary. *Bull. Mar. Sci.* 91, 323–341. <https://doi.org/10.5343/bms.2014.1060>.
94. Smyth, A.R., Gerald, N.R., Thompson, S.P., and Piehler, M.F. (2016). Biological activity exceeds biogenic structure in influencing sediment nitrogen cycling in experimental oyster reefs. *Mar. Ecol. Prog. Ser.* 560, 173–183. <https://doi.org/10.3354/meps11922>.
95. Sanford, R.A., Wagner, D.D., Wu, Q., Chee-sanford, J.C., Thomas, S.H., Cruz-garcía, C., Rodríguez, G., Massol-Deyá, A., Krishnani, K.K., Ritalahti, K.M., et al. (2012). Unexpected nondenitrifier nitrous oxide reductase gene diversity and abundance in soils. *Proc Natl Acad Sci* 109, 19709–19714. <https://doi.org/10.1073/pnas.1211238109>.
96. Jones, C.M., Graf, D.R.H., Bru, D., Philippot, L., and Hallin, S. (2013). The unaccounted yet abundant nitrous oxide-reducing microbial community: A potential nitrous oxide sink. *ISME J.* 7, 417–426. <https://doi.org/10.1038/ismej.2012.125>.
97. Hallin, S., Philippot, L., Löffler, F.E., Sanford, R.A., and Jones, C.M. (2018). Genomics and Ecology of Novel N2O-Reducing Microorganisms. *Trends Microbiol.* 26, 43–55. <https://doi.org/10.1016/j.tim.2017.07.003>.
98. Orellana, L.H., Rodriguez-R, L.M., Higgins, S., Chee-Sanford, J.C., Sanford, R.A., Ritalahti, K.M., Löffler, F.E., and Konstantinidis, K.T. (2014). Detecting nitrous oxide reductase (nosZ) genes in soil metagenomes: method development and implications for the nitrogen cycle. *mBio* 5, e01193. <https://doi.org/10.1128/mbio.01193-14>.
99. Smith, C.J., Nedwell, D.B., Dong, L.F., and Osborn, A.M. (2007). Diversity and abundance of nitrate reductase genes (narG and napA), nitrite reductase genes (nirS and nrfA), and their transcripts in estuarine sediments. *Appl. Environ. Microbiol.* 73, 3612–3622. <https://doi.org/10.1128/AEM.02894-06>.
100. Mara, P., Edgcomb, V.P., Sehein, T.R., Beaudoin, D., Martinsen, C., Lovely, C., Belcher, B., Cox, R., Curran, M., Farnan, C., et al. (2021). Comparison of Oyster Aquaculture Methods and Their Potential to Enhance Microbial Nitrogen Removal From Coastal Ecosystems. *Front. Mar. Sci.* 8, 1–23. <https://doi.org/10.3389/fmars.2021.633314>.
101. Babraham Bioinformatics (2020). FastQC. <https://www.bioinformatics.babraham.ac.uk/projects/fastqc/>.
102. Martin, M. (2011). Cutadapt removes adapter sequences from high-throughput sequencing reads. *EMBnet J.* 17, 10. <https://doi.org/10.14806/ej.17.1.200>.
103. Bolger, A.M., Lohse, M., and Usadel, B. (2014). Trimmomatic: a flexible trimmer for Illumina sequence data. *Bioinformatics* 30, 2114–2120. <https://doi.org/10.1093/bioinformatics/btu170>.
104. Clarke, E.L., Taylor, L.J., Zhao, C., Connell, A., Lee, J.J., Fett, B., Bushman, F.D., and Bittinger, K. (2019). Sunbeam: an extensible pipeline for analyzing metagenomic sequencing experiments. *Microbiome* 7, 46. <https://doi.org/10.1186/s40168-019-0658-x>.
105. Wood, D.E., Lu, J., and Langmead, B. (2019). Improved metagenomic analysis with Kraken 2. *Genome Biol.* 20, 257. <https://doi.org/10.1186/s13059-019-1891-0>.
106. Silva, G.G.Z., Green, K.T., Dutilh, B.E., and Edwards, R.A. (2016). SUPER-FOCUS: a tool for agile functional analysis of shotgun metagenomic data. *Bioinformatics* 32, 354–361. <https://doi.org/10.1093/bioinformatics/btv584>.
107. Looft, T., Johnson, T.A., Allen, H.K., Bayles, D.O., Alt, D.P., Stedtfeld, R.D., Sul, W.J., Stedtfeld, T.M., Chai, B., Cole, J.R., et al. (2012). In-feed antibiotic effects on the swine intestinal microbiome. *Proc. Natl. Acad. Sci. USA* 109, 1691–1696. <https://doi.org/10.1073/pnas.1120238109>.
108. Krakau, S., Straub, D., Gourel, H., Gabernet, G., and Nahnsen, S. (2022). nf-core/mag: a best-practice pipeline for metagenome hybrid assembly and binning. *NAR Genom. Bioinform.* 4, lqac007. <https://doi.org/10.1093/nargab/lqac007>.
109. Chen, S., Zhou, Y., Chen, Y., and Gu, J. (2018). fastp: an ultra-fast all-in-one FASTQ preprocessor. *Bioinformatics* 34, i884–i890. <https://doi.org/10.1093/bioinformatics/bty560>.
110. Prjibelski, A., Antipov, D., Meleshko, D., Lapidus, A., and Korobeynikov, A. (2020). Using SPAdes De Novo Assembler. *Curr. Protoc. Bioinformatics* 70, e102. <https://doi.org/10.1002/cpbi.102>.
111. Kang, D.D., Li, F., Kirton, E., Thomas, A., Egan, R., An, H., and Wang, Z. (2019). MetaBAT 2: an adaptive binning algorithm for robust and efficient genome reconstruction from metagenome assemblies. *PeerJ* 7, e7359. <https://doi.org/10.7717/peerj.7359>.
112. Simão, F.A., Waterhouse, R.M., Ioannidis, P., Kriventseva, E.V., and Zdobnov, E.M. (2015). BUSCO: assessing genome assembly and annotation completeness with single-copy orthologs. *Bioinformatics* 31, 3210–3212. <https://doi.org/10.1093/bioinformatics/btv351>.
113. Gurevich, A., Saveliev, V., Vyahhi, N., and Tesler, G. (2013). QUAST: quality assessment tool for genome assemblies. *Bioinformatics* 29, 1072–1075. <https://doi.org/10.1093/bioinformatics/btt086>.
114. Chaumeil, P.A., Mussig, A.J., Hugenholtz, P., and Parks, D.H. (2019). GTDB-Tk: a toolkit to classify genomes with the Genome Taxonomy Database. *Bioinformatics* 36, 1925–1927. <https://doi.org/10.1093/bioinformatics/btz848>.
115. Seemann, T. (2014). Prokka: rapid prokaryotic genome annotation. *Bioinformatics* 30, 2068–2069. <https://doi.org/10.1093/bioinformatics/btu153>.
116. Asnicar, F., Thomas, A.M., Beghini, F., Mengoni, C., Manara, S., Manghi, P., Zhu, Q., Bolzan, M., Cumbo, F., May, U., et al. (2020). Precise phylogenetic analysis of microbial isolates and genomes from metagenomes using PhyloPhlAn 3.0. *Nat. Commun.* 11, 2500. <https://doi.org/10.1038/s41467-020-16366-7>.
117. Stamatakis, A. (2014). RAxML version 8: a tool for phylogenetic analysis and post-analysis of large phylogenies. *Bioinformatics* 30, 1312–1313. <https://doi.org/10.1093/bioinformatics/btu033>.
118. Tu, Q., Lin, L., Cheng, L., Deng, Y., and He, Z. (2019). NCycDB: a curated integrative database for fast and accurate metagenomic profiling of nitrogen cycling genes. *Bioinformatics* 35, 1040–1048. <https://doi.org/10.1093/bioinformatics/bty741>.
119. Buchfink, B., Reuter, K., and Drost, H.G. (2021). Sensitive protein alignments at tree-of-life scale using DIAMOND. *Nat. Methods* 18, 366–368. <https://doi.org/10.1038/s41592-021-01101-x>.

STAR★METHODS

KEY RESOURCES TABLE

REAGENT or RESOURCE	SOURCE	IDENTIFIER
<b>Biological samples</b>		
Diploid and Triploid Oysters	This study	N/A
<b>Critical commercial assays</b>		
Qiagen MagAttract PowerSoil DNA KF kit	<a href="https://www.qiagen.com/us/products/">https://www.qiagen.com/us/products/</a>	Cat. No./ID: 27100-4-EP
LightCycler 480 SYBR Green I Master	Roche Life Science( <a href="https://lifescience.roche.com/global/en/products/">https://lifescience.roche.com/global/en/products/</a> )	Cat # 04707516001
<b>Deposited data</b>		
Shallow shotgun metagenomic sequences	This paper	NCBI: PRJNA858118, Biosample #SAMN29671270 to SAMN29671291 and SRA#SRS13888819
<b>Experimental models: Organisms/strains</b>		
<i>Crassostrea virginica</i>	Aquaculture research lease of the Wakulla Environmental Institute located in Oyster Bay	Taxonomic Serial Number (TSN):79872
<b>Software and algorithms</b>		
Fast QC v0.11.5	Babraham Bioinformatics <sup>101</sup>	<a href="https://www.bioinformatics.babraham.ac.uk/projects/fastqc/">https://www.bioinformatics.babraham.ac.uk/projects/fastqc/</a>
Cutadapt v2.6	Martin et al. <sup>102</sup>	<a href="https://doi.org/10.14806/ej.17.1.200">https://doi.org/10.14806/ej.17.1.200</a>
Trimmomatic v0.36	Bolger et al. <sup>103</sup>	<a href="https://doi.org/10.1093/bioinformatics/btu170">https://doi.org/10.1093/bioinformatics/btu170</a>
Komplexity v0.3.6	Clarke et al. <sup>104</sup>	<a href="https://doi.org/10.1186/s40168-019-0658-x">https://doi.org/10.1186/s40168-019-0658-x</a>
Kraken2	Wood et al. <sup>105</sup>	<a href="https://doi.org/10.1186/s13059-019-1891-0">https://doi.org/10.1186/s13059-019-1891-0</a>
Super-Focus	Silva et al. <sup>106</sup>	<a href="https://doi.org/10.1093/bioinformatics/btv584">https://doi.org/10.1093/bioinformatics/btv584</a>
nf-core/MAG pipeline v2.1.1	Krakau et al. <sup>107</sup>	<a href="https://doi.org/10.1093/nargab/lqac007">https://doi.org/10.1093/nargab/lqac007</a>
Fastp v0.20.1	Chen et al. <sup>108</sup>	<a href="https://doi.org/10.1093/bioinformatics/bty560">https://doi.org/10.1093/bioinformatics/bty560</a>
SPAdesv3.15.3	Prijbelski et al. <sup>109</sup>	<a href="https://doi.org/10.1002/cpbi.102">https://doi.org/10.1002/cpbi.102</a>
Meta BAT2 v2.15	Kang et al. <sup>110</sup>	<a href="https://doi.org/10.7717/peerj.7359">https://doi.org/10.7717/peerj.7359</a>
BUSCO v5.1.0	Simao et al. <sup>111</sup>	<a href="https://doi.org/10.1093/bioinformatics/btv351">https://doi.org/10.1093/bioinformatics/btv351</a>
Quast v5.0.2	Gurevich et al. <sup>112</sup>	<a href="https://doi.org/10.1093/bioinformatics/btt086">https://doi.org/10.1093/bioinformatics/btt086</a>
GT-DB-TK v1.5.0	Chaumeil et al. <sup>113</sup>	<a href="https://doi.org/10.1093/bioinformatics/btz848">https://doi.org/10.1093/bioinformatics/btz848</a>
Prokka v1.14.6	Seemann. <sup>114</sup>	<a href="https://doi.org/10.1093/bioinformatics/btu153">https://doi.org/10.1093/bioinformatics/btu153</a>
PhyloPhlAn v3.0.67	Asnicar et al. <sup>115</sup>	<a href="https://doi.org/10.1038/s41467-020-16366-7">https://doi.org/10.1038/s41467-020-16366-7</a>
Rax ML v1.33	Stamatakis et al. <sup>116</sup>	<a href="https://doi.org/10.1093/bioinformatics/btu033">https://doi.org/10.1093/bioinformatics/btu033</a>
FastANI v1.33	Jain et al. <sup>87</sup>	<a href="https://doi.org/10.1038/s41467-018-07641-9">https://doi.org/10.1038/s41467-018-07641-9</a>
NCycDB	Tu et al. <sup>117</sup>	<a href="https://doi.org/10.1093/bioinformatics/bty741">https://doi.org/10.1093/bioinformatics/bty741</a>
DIAMOND v2.0.14.152	Buchfink et al. <sup>118</sup>	<a href="https://doi.org/10.1038/s41592-021-01101-x">https://doi.org/10.1038/s41592-021-01101-x</a>

## RESOURCE AVAILABILITY

### Lead contact

Further information and requests for resources and reagents should be directed to the [lead contact](#), Dr. Ashvini Chauhan ([ashvini.chauhan@famu.edu](mailto:ashvini.chauhan@famu.edu)).

### Materials availability

This study did not generate new unique reagents or materials.

### Data and code availability

Standardized shallow shotgun metagenomics sequences have been deposited at NCBI and are publicly available. Accension numbers are listed in the [key resources table](#).

This paper does not report original codes.

Any additional information required to reanalyze the data reported in this paper is available from the [lead contact](#).

## METHOD DETAILS AND BIOINFORMATICS

Sample collection, DNA Extraction and Library Preparation for Next-Generation Sequencing (NGS), DNA Sequencing, Quality Control Analysis, Data Curation, and Sequence Processing, HT-qPCR Quantitative Microbial Element Cycling (QMEC), Metagenome Assembled Genomes (MAGs), Phylogenetic Analysis of Binned Metagenomes, Average Nucleotide Identity (ANI) Analysis of MAGs, Identification of Denitrification Genes in MAGs and RefSeq Genomes, Shallow Shotgun Metagenome Submission: Metagenomic Sequence Accession Numbers.

### Sample collection, experimental model, and study participant details

Cultured *C. virginica* were collected from the aquaculture research lease of the Wakulla Environmental Institute located in Oyster Bay [30.0342702, -84.3558844], near Panacea, Florida. Oysters were grown in plastic cages, suspended from lines attached to pilings at depths of 1–2 m (Australian Adjustable Long-Line System; <https://seapa.com.au/farming-systems/>). At each sampling time from December 2016–August 2017, representative of the warm and cold seasons in North Florida (Panacea), diploid and triploid oysters grown in adjacent cages were sampled monthly from the Wakulla Environmental Institute Research Aquaculture lease site in Oyster Bay, near Panacea Florida, stored in Ziploc bags over ice for ~45 min for their transportation from the site to the FAMU laboratory, where they were immediately stored in a –80°C freezer until being processed for DNA analysis. Oysters were measured using digital calipers to ensure only adults are harvested, by measuring the shell height as the maximum distance from umbo (hinge) to lip (commissure) (per Galtsoff, P. S. 1964. The American Oyster *Crassostrea virginica* Gmelin (Fishery Bulletin, v. 64. United States Government Printing Office, Washington, D. C.). For DNA extraction 6 diploid and 6 triploid oysters were thawed, shucked, and pooled by ploidy for each monthly sampled time point. Duplicate samples were then aliquoted and used for sequencing.

### DNA extraction and library preparation for next-generation sequencing

Prior to the opening of bivalves, each oyster was first externally rinsed with sterile water and scrubbed thoroughly to remove the shell biofilm. They were then opened with a shucking knife at the hinge where the adductor muscle is located joining the two shells. Once opened, the oyster's mantle fluid was drained, and the entire oyster was collected. Pooled ( $n = 6$ ) each of diploid and triploid oysters, from each time point, were then homogenized thoroughly using the Oster brand kitchen blender and processed for DNA extraction.

At each time, 250 mg of homogenized oyster tissues were used to extract DNA in duplicate, labeled as A and B, using the Qiagen MagAttract PowerSoil DNA KF kit (Formerly MOBio PowerSoil DNA Kit). DNA quality was evaluated visually via gel electrophoresis and quantified using a Qubit 3.0 fluorometer (Thermo-Fischer, Waltham, MA, USA). Libraries were then prepared by MicrobiomeInsights Inc. (<https://microbiomeinsights.com/>) using an Illumina Nextera library preparation kit using their in-house protocol (Illumina, San Diego, CA, USA).

### DNA sequencing, quality control analysis, data curation, and sequence processing

Paired-end sequencing (150 bp × 2) was done on a NextSeq 500 in medium-output mode. Shotgun metagenomic sequence reads were processed with the Sunbeam pipeline. Initial quality evaluation was done using FastQC v0.11,<sup>101</sup> followed by adapter removal, read trimming, low-complexity-reads removal, and host-sequence removals. Adapter removal was done using cutadapt v2.6<sup>102</sup> and trimming was done with Trimmomatic v0.36<sup>103</sup> using custom parameters (leading 3, trailing 3, sliding window 4:15, minimum length 36). Low-quality sequences were detected with Komplexity v0.3.6<sup>104</sup> and discarded from further analysis. High-quality reads were mapped to the human genome (Genome Reference Consortium Human ref. 37) and to the *Crassostrea virginica* genome v3.0 (Accession number GCF\_002022765.2); matching sequences were removed (labeled as host in [Figure SI-1](#)), along with low quality reads (marked as low quality in [Figure SI-1](#)), respectively. Among the high-quality reads, six sequenced samples were considered outliers because they contained a variable number of host reads. These samples, represented by  $n = 6$  pooled oysters included triploid oysters from January (010717 Triploid A and 010717 Triploid B), Diploid B oysters from May (051117), Diploid A oysters from December 2016 (120516), and both duplicate triploids from December 2016 (120516).

Triploid A, and 120516 Triploid B), respectively (note that samples are labeled based on their collection date and ploidy). To retain the high quality read samples, we subsampled five of them to the median value of reads for the non-outliers (6768 reads). Sample 051117 Diploid B had a similar number of reads to the other samples, so it was not subsampled. The remaining reads, marked as retained in Figure SI-1, were taxonomically classified using Kraken2<sup>105</sup> with the minikraken v1 database. Functional profiles were not subsampled, and the five outliers were removed from the downstream bioinformatics analysis. For functional profiling, high-quality (filtered) reads were aligned against the SEED database via translated homology search and annotated to subsystems, or functional levels, 1–3 using Super-Focus.<sup>106</sup>

### High-throughput- quantitative microbial element cycling

Based on high-throughput qPCR (HT-qPCR), a recently developed method called QMEC [Quantitative Microbial Elemental Cycling (QMEC)], has the potential to simultaneously detect and quantify biogeochemical cycling genes for C, N, P and S, thus providing a deeper understanding on these microbially mediated processes.<sup>51</sup> Briefly, a total of 72 primer sets were used to quantify DNA extracted from homogenized oyster samples. The primer sets targeted the 16S ribosomal RNA (rRNA) gene, and 35 carbon cycling genes (C), 22 nitrogen cycling genes (N), 9 phosphorus cycling genes (P) and 5 sulfur cycling genes (S). Amplification for each sample was conducted in triplicates, using 100 nL containing (final concentration) 1 × Light Cycler 480 SYBR Green I Master Mix (Roche Inc., USA), nuclease free PCR-grade water, 1–3 ng  $\mu\text{L}^{-1}$  DNA template, and 1  $\mu\text{M}$  each of forward and reverse primers. High-throughput qPCR (HT-qPCR) was performed by the Smart Chip Real-time PCR system (Takara Bio USA, Inc.). A non-template negative control was set for each primer set. The thermal cycle curve conditions included an initial denaturation at 95°C for 10 min with 40 cycles of denaturation at 95°C for 30 s, annealing at 58°C for 30 s, and extension at 72°C for 30 s. The melting curve analysis was automatically generated by the software, and the qPCR results were analyzed using Smart Chip qPCR software. Samples with efficiencies beyond the range of 1.7–2.3 or an  $r^2$  under 0.99 were discarded. A threshold cycle (Ct) 31 was used as the detection limit. All three replicates that amplified successfully were used for further data analysis. The relative gene copy number was calculated as described by Looft et al.<sup>107</sup> using following equation.

$$\text{Relative copy number} = 10^{((31-CT)/(10/3))}$$

where CT refers to HT-qPCR results, 31 refers to the detection limit.

Absolute 16S rRNA copy numbers were determined by the standard curve (SC) method of quantification using the Roche 480 system. Each 20  $\mu\text{L}$  qPCR consisted of 10  $\mu\text{L}$  2× Light Cycle 480 SYBR Green I Master (Roche Applied Sciences), 1  $\mu\text{M}$  each primer, 2–6 ng DNA as template and enough nuclease-free PCR-grade water. The thermal cycle consisted of 5 min initial enzyme activation at 95°C, followed by 40 cycles of denaturation at 95°C for 30 s, annealing at 60°C for 30 s, and extension 72°C for 20 s. A plasmid control containing a cloned and sequenced 16S rRNA gene fragment ( $6.69 \times 10^8$  copies per microliter) was used to generate five-point calibration curves from 10-fold dilutions. All qPCRs were performed in technical triplicates with non-template reactions serving as a negative control.

### Metagenome assembled genomes

Metagenomes were assembled, binned into MAGs (metagenome-assembled genomes), and annotated using the nf-core/mag pipeline v2.1.1.<sup>108</sup> Raw reads from 22 samples were used as input. Reads were trimmed using fastp v0.20.1<sup>109</sup> and assembled using SPAdes v3.15.3.<sup>110</sup> Metagenomic contigs were grouped into draft genomes (i.e., binned into MAGs) using MetaBAT 2 v2.15.<sup>111</sup> Bin quality was assessed using BUSCO v5.1.0<sup>112</sup> and Quast v5.0.2.<sup>113</sup> Bins with a level of completeness less than 15% (based on BUSCO results) were excluded from further analysis. Taxonomic classification of bins was performed using GTDB-Tk v1.5.0.<sup>114</sup> Bins were annotated using Prokka v1.14.6.<sup>115</sup>

### Phylogenetic analysis of binned metagenomes

Prokka-derived protein sequences from four metagenomic bins classified as *Psychrobacter* were used to construct a phylogenetic tree, using PhyloPhlAn v3.0.67.<sup>116</sup> 215 RefSeq *Psychrobacter* proteomes available in the NCBI Assembly database were downloaded and included in the analysis, as well as a *Moraxella lincolnii* protein set (GCF\_002014765.1), for use as an outgroup. The “phylophlan” database of 400 universal marker genes was used, and a diversity setting of “medium” was specified. RAxML v 8.2.12<sup>117</sup> was used to generate a maximum likelihood tree with bootstrap values from 100 replicates.

### Average nucleotide identity analysis of metagenome assembled genomes

Whole-genome similarity between each *Psychrobacter* MAG and all NCBI RefSeq *Psychrobacter* genomes was assessed by ANI, and calculated using FastANI v1.33.<sup>87</sup> For the ANI analysis all RefSeq *Psychrobacter* assemblies were compared to each MAG. A separate ANI result was generated for each comparison, providing a total of 993 ANI values. For each MAG the highest ANI was identified and that RefSeq sequence is reported. No minimum ANI threshold was used in this process.

### Identification of denitrification genes in metagenome assembled genomes and RefSeq genomes

Prokka-derived proteins for *Psychrobacter* MAGs and protein sequences from NCBI for similar *Psychrobacter* RefSeq genomes (based on ANI) were analyzed for denitrification genes using NCycDB.<sup>118</sup> Searching was performed against the NCyc\_100.faa database using DIAMOND v2.0.14.152.<sup>119</sup> The following genes/proteins were assessed: *napA* (Periplasmic nitrate reductase NapA), *napB* (Cytochrome c-type protein NapB), *narG* (Nitrate reductase), *narH* (Nitrate reductase), *narI* (Nitrate reductase gamma subunit), *nirK* (Nitrite reductase),

*nirS* (Nitrite reductase), *norB* (Nitric oxide reductase subunit B), *norC* (Nitric oxide reductase subunit C), *nosZ* (Nitrous-oxide reductase). NCycDB results were compared to Prokka and NCBI annotations, and additional BLAST searches against the NCBI RefSeq and UniProtKB/Swiss-Prot databases were performed to resolve conflicting functional assignments.

### Shallow shotgun metagenome submission: metagenomic sequence accession numbers

The shallow shotgun metagenomic sequences obtained from this study are available under NCBI accession # PRJNA858118, Biosample #SAMN29671270 to SAMN29671291 and SRA#SRS13888819 to SRS13888833(<https://www.ncbi.nlm.nih.gov/bioproject/PRJNA858118/>).

- (1) Data Transformation and Statistical Analysis
  - Summary of Data Transformation
  - Statistical Analysis

### Summary of data transformation

All qPCR data was normalized into relative and absolute abundance. The relative abundance was calculated by normalizing the relative gene copy of each C, N, P, and S-cycling genes with its relative 16S copy number (equation I).<sup>51</sup> The absolute abundance was calculated by multiplying the 16S copy number with the relative abundance of each C, N, P, and S-cycling genes and dividing the product with its respective DNA concentration (equation II).<sup>51</sup> The calculated absolute abundance was then normalized into copies/g oyster among samples (equation III),<sup>51</sup> which was used to evaluate the total CNPS genes in each sample.

### Statistical analysis

Averages and standard deviations were calculated in Microsoft Excel. Statistical visualizations were done in R and Origin statistical software. Heatmaps, correlation, hierarchical clustering analysis, and were done on R studio (<https://www.R-project.org/>) using pheatmap, vegan, corrplot, and ggplot 2. The stacked bar charts were plotted in Origin (<https://www.originlab.com/>).

Negative binomial models (DESeq2 R package) were used for the differential abundance testing of taxonomic and subsystem level features. Changes due to sampling timepoint differences after controlling for genotype differences (ploidy) were analyzed; because we did not notice major differences between genotypes by PERMANOVA, we used all samples together even though several timepoints were missing for the diploid samples. We plotted the top 20 groups for each test, based on their adjusted *p*-values, which were calculated using the likelihood ratio test (LRT). The critical *p*-value (alpha value) were used to compare the adjusted *p*-values (=0.01) of the multiple independent groups, unless otherwise stated.

Furthermore, the abundance of the top 10 bacterial taxa and gene functions were averaged to produce a single dataset for each sampling time point representing diploids or triploid samples which was then imported into the Primer-E software suite (version 6.1.18; PRIMER-E, Ivy-bridge, United Kingdom). Normalization of data was performed using the log (*X*+1) pre-treatment function in the Primer-E software and after transformation, a Bray-Curtis similarity matrix was generated, and non-metric multidimensional scaling plot (NMDS) was obtained using parameters of Kruskal stress formula1 and minimum stress 0.01. Dendrogram analysis was performed based on the group average option using Primer-E software.